RESPONSE TO TIDES OF COASTAL AQUIFERS: ANALOG SIMULATION VS. FIELD OBSERVATION

by

John A. Williams
Ta-Chiang Liu

Technical Report No. 86

June 1975

Project Completion Report
for
ANALOG SIMULATION OF TIDAL EFFECTS

OWRT Project No. A-020-HI, Grant Agreement No. 14-31-0001-3511
Principal Investigator: John A. Williams
Project Period: July 1, 1970 to August 31, 1972

The programs and activities described herein were supported in part by funds provided by the United States Department of the Interior as authorized under the Water Resources Act of 1964, Public Law 88-379.

ABSTRACT

This report presents a summary of the work to date on the response to tides of coastal aquifers. In particular, it presents the results of experiments performed to study the influence of an oscillating water table on storativity (i.e., effective porosity), the application of both harmonic and spectral analyses to water surface time histories measured in the field near Ewa Beach and in Honolulu Harbor, and an electric analog model designed to simulate the shallow, coral-limestone aquifer at Ewa Beach, Oahu, Hawaii. Results indicate that the effective porosity for an oscillating water table will, in general, depend on the frequency of the oscillation with dependence being strong or weak as either or both the specific yield and the transmissivity are larger or smaller, respectively. Also, water surface time histories can be considered to be composed of a fundamental (diurnal) component and a second harmonic (semidiurnal) component and a 24-hr record analyzed and that the resulting average values of the amplitude and phase angles be used. The spectral analysis confirms that the semidiurnal power suffers a greater attenuation than the diurnal power.

It is concluded that the technique of determining aquifer properties from tidal response data is a valid one, but that the results will be less reliable than those ascertained from pump test data. The optimum results are considered to be those based on both tidal data and pump test data, as one method serves as a check on the other.

CONTENTS

FIGURES

TABLES

INTRODUCTION

The Water Resources Research Center at the University of Hawaii in 1968 undertook a research program to study the response of coastal aquifers to tidal fluctuation. In particular, it was desired to determine the feasibility of using tidal response data to help determine aquifer properties. The first phase of the program (OWRT Proj. No. A-015-HI) dealt essentially with modeling techniques, mathematical, electric analog, and hydraulic, and verified the use of the diffusion theory for representation of the physical phenomena involved, provided the appropriate diffusion coefficients were used (Williams, Wada, and Wang 1970).

The results of this initial research provided the impetus for the second study (OWRT Proj. No. A-020-HI) which was conducted in two phases. The first phase concentrated on the development of mathematical models and the corresponding electric analog models for several specific cases of inhomogeneity (Williams and Liu 1971) and for an aquifer system in which leakage was involved (Williams and Liu 1973). The second phase was an attempt to apply the results of the previous work in the construction of an electric analog model of a real aquifer and to verify the model using tidal response data as well as additional information, such as pumping test data, if available.

For all of the models mentioned above, an isotropic shallow aquifer in direct communication with the sea was assumed. However, in Hawaii the primary basal aquifer is quite deep, perhaps as much as 3000 to 5000 ft (Williams and Soroos 1973), which renders the application of the shallow aquifer theory questionable. To investigate this aspect, an additional study was conducted simultaneously with Phases I and II which employed a vertical Hele-Shaw flow model to simulate an unconfined aquifer (Liu 1973). The observations of the tidal response in the model, for a range of increasing depths, were compared with the shallow aquifer theory based on the Dupuit assumptions as well as with the deep aquifer response to tidal fluctuations as derived by Carrier and Munk (1952).

It is the purpose of this report to present the results of the second phase of the work described above and to relate these results to those of previous and current pertinent work.

SHORT TERM FLUCTUATIONS IN THE PIEZOMETRIC SURFACE

The piezometric surface in an aquifer is subject to periodic fluctuations from a variety of sources. Three such sources are fluctuations in barometric pressure, earth tides, and ocean tides. Usually several of these influences are acting simultaneously and are superposed on the longer term seasonal fluctuations.

Fluctuations Caused by Barometric Pressure Changes

Confined aquifer response to barometric pressure fluctuations is characterized by a 180° phase difference with respect to the pressure change. Thus, increases in barometric pressure depress the piezometric head and vice-versa. The barometric efficiency, b.e., of an aquifer is defined as the ratio of a change in barometric pressure, Δp_o, to the corresponding change in the piezometric head. Jacob (1940) related this ratio to the bulk modulus of the water, β_w, the elastic modulus of the granular skeleton, E_s, and the porosity of the media, ε. The derivation assumes that the change in barometric pressure is supported partially by the water in the pore space and by the solid skeleton and that the water and the skeleton obey Hooke's law in such a way that the volume changes in both are the same (i.e., the individual solid particles in the skeleton do not change in volume).[1] The resulting relation is

$$\text{b.e.} = \frac{\gamma \Delta h}{\Delta p_o} = \frac{\Delta p - \Delta p_o}{\Delta p_o} = \frac{\Delta \sigma_s}{\Delta \sigma_s + \Delta p} = \frac{1}{1 + \frac{\Delta p}{\Delta \sigma_s}} \tag{1}$$

where σ_s and p are the compressive stresses in the skeleton and the water, respectively. If the condition of equal changes in volume together with Hooke's law for the water and the skeleton are applied to equation (1), the result is

$$\text{b.e.} = \frac{\varepsilon E_s}{\varepsilon E_s + \beta_w} \tag{2}$$

The utility of the barometric efficiency is found in the fact that it may be related to the storativity of the aquifer. Following Todd (1964), the compressibility of the aquifer is taken as the compressibility of the

1. For the case where this latter assumption is not made, see Tuinzaad (1954).

water plus the compressibility of the skeleton. Thus, if volume changes are with respect to a unit volume of aquifer,[1]

$$\frac{1}{E_{aq}} = \frac{\varepsilon}{\beta_w} + \frac{1}{E_s} = \frac{\varepsilon}{\beta_w(b.e.)} \tag{3}$$

Finally, since the storativity is defined as the volume of fluid per unit column of aquifer released under a unit decline in head, i.e., $S=\gamma b/E_{aq}$, then

$$S = \frac{\varepsilon\gamma b}{\beta_w(b.e.)} \tag{4}$$

where b is the aquifer thickness.

Aquifer response to barometric pressure fluctuations has been well documented by Robinson (1939) and others (Nilsson 1966).

Fluctuations Caused by Ocean Tides

The ocean tides consist of a complex wave system composed of a number of harmonic constituents. Eight of the more important constituents have been identified by Defant (1958) and are presented in Table 1 below.

TABLE 1. SIGNIFICANT COMPONENTS OF A REAL OCEAN TIDE

SYMBOL	PERIOD IN SOLAR HOURS	RELATIVE AMPLITUDE	DESCRIPTION OF COMPONENT
M_2	12.42	100	MAIN LUNAR (SEMIDIURNAL CONSTITUENT)
S_2	12.00	46.6	MAIN SOLAR (SEMIDIURNAL CONSTITUENT)
N_2	12.66	19.1	LUNAR CONSTITUENT DUE TO MONTHLY VARIATION IN MOON'S DISTANCE
K_2	11.97	12.7	SOLI-LUNAR CONSTITUENT DUE TO CHANGES IN DECLINATION OF SUN AND MOON
K_1	23.93	58.4	SOLI-LUNAR
O_1	25.82	41.5	MAIN LUNAR
P_1	24.07	19.3	MAIN SOLAR
M_f	327.86	17.2	FORTNIGHTLY-LUNAR

SOURCE: DEFANT 1958.

1. A more accurate expression is $1/E_{aq}=\varepsilon/\beta_w+(1-\varepsilon)/E_s$. However, eq. (3) is considered to be consistent with the accuracy of the shallow-aquifer approximations. See Bear 1972.

If a fundamental period of 670 hr (i.e., 28 days less 2 hr) is divided into its harmonics, then periods of 25.77, 23.97, 12.64, 12.41, and 11.96 hr correspond to the harmonic numbers 26, 28, 53, 54, and 56, respectively. These periods agree very closely with those of the diurnal and semidiurnal tidal constituents. Thus, the harmonic analysis of a record of 670 hr duration will yield the amplitudes of 5 components which will correspond to the O_1, p_1 plus K_1, H_2, M_2, and S_2 plus K_2 tidal constituents. This technique was first described by Doodson (1922).

The problem of periodic fluctuations produced by ocean tides can be separated into two categories: the first is that where the aquifer is in direct communication with the sea by virtue of its outcrop at the coastline, and the second is that where the aquifer is confined and the confining layer is overlain completely or partially by a body of water subject to tidal fluctuations. Within this latter category is a class of more complicated problems in which there exist breaks in the aquitard permitting direct interaction between the aquifer and the overlying ocean.

AQUIFERS COMMUNICATING DIRECTLY WITH THE SEA. The simplest case consists of a one-dimensional flow in a shallow, homogeneous and isotropic aquifer bounded by a vertical coastline at one end and extending to infinity in the direction of x. The solution of the basic (diffusion) differential equation gives

$$h(x,t) = \zeta_o e^{-\alpha x} \sin(\alpha x - \sigma t);\ \alpha = \sqrt{\frac{S\sigma}{2T}} \qquad (5a)$$

where ζ_o is the tidal amplitude, $\sigma = 2\pi/t_o$ is the frequency of a particular tidal component, α is the damping factor and h is the piezometric head. From equation (5a) the wave length and speed of the disturbance in the aquifer are, respectively,

$$\lambda = \frac{2\pi}{\alpha} = \sqrt{\frac{4\pi T t_o}{S}} \qquad (5b)$$

and

$$C = \frac{\sigma}{\alpha} = \sqrt{\frac{4\pi T}{S t_o}} \qquad (5c)$$

The wave length, λ, is also referred to as the "penetration length" and is that distance from the coastline where the fluctuation in the piezometric

is in phase with the tide at the coastline.

It is clear that the response to a given tidal component observed in a well at a known distance from the coastline, together with the amplitude of the tidal component, will permit a calculation of α and a subsequent estimate of the ratio, S/T, provided the period is also known.

AQUIFERS COMMUNICATING INDIRECTLY WITH THE SEA. The case of a confined aquifer overlain by a body of water subject to tidal fluctuations was first investigated by Jacob (1941). Jacob defined the tidal efficiency as the ratio of the change in piezometric head in the aquifer to the corresponding change in the elevation of the overlying sea water. Thus, using the same assumptions concerning the relative roles of the water and the granular skeleton as in the calculations for the barometric efficiency, the result is

$$\text{t.e.} = \frac{\Delta p/\sigma}{\Delta H} = \frac{\Delta p}{\Delta p + \Delta r_s} = \frac{1}{1 + \frac{\Delta \sigma_s}{\Delta p}} = \frac{1}{1 + \frac{\varepsilon E_s}{\beta_w}} \tag{6}$$

It is clear from equations (1) and (6) that

$$\text{b.e.} + \text{t.e.} = 1 \tag{7}$$

and that

$$S = \frac{\varepsilon \alpha b}{\beta_w (1 - \text{t.e.})} \tag{8}$$

Fluctuations Caused by Earth Tides

The gravitational attraction between the earth and the moon and the earth and the sun generates a land tide as well as an ocean tide. The effect of a land tide on a confined groundwater body is such that for "high tide" the piezometric surface declines and for "low tide" it rises. This is the result of the aquifer overburden weighing less at "high tide", i.e., when the moon is at upper or lower culmination, than at low tide, when the moon is on the horizon.[1] The fluctuation of the piezometric surface resulting from earth tides has been well documented by Robinson (1909), and by B. Gustafsson and M. Nordstrom in Nilsson (1966). According to Dale

1. The influence of the land tide was noted as early as the first century by Pliny the Elder in his *Historia Naturalis* in which he notes that "the water in a well rises and falls as in the sea but at other times." See Nilsson (1966).

(1974), earth tides do not noticeably influence the groundwater tides in Hawaii.

REVIEW OF PERTINENT RESEARCH WORK

Aquifers in Direct Communication with the Sea

Work on the tidal response problem dates back at least to Boussinesq (1904) who solved the basic differential equation which bears his name and arrived at the solution given in equation (5). Werner and Noren (1951) extended this solution to include the case of an aquifer of finite length and compared their results with field observations by Prinz (1923). The field data shows a variation in head, h, consistent with equation (5) provided the fluctuations in head at the river (i.e., at x=0) are ignored. The data are presented in Figure 1.

Williams, Wada, and Wang (1970) recast the more general solution of Werner and Noren (1951) into a form more accessible to digital computations and extended it to include a constant head as well as a no-flow condition at the interior boundary of the aquifer. Their results include a comparison of this mathematical model against both an electric analog model and an hydraulic model which employed polyurethene foam as the porous elastic skeleton. Specifically, amplitude and phase angles of the fluctuations were measured at several points in the hydraulic model. The measured amplitudes, the distance to the point of observation, and the tidal period were then substituted into the mathematical model and values of α at each observation position calculated. With α known, the ratio of storativity to transmissivity was estimated.

Since the value of the conductivity depends on the structure of the porous media for a given fluid at a constant temperature, it was concluded that variations in α were essentially variations in the storativity. With the conductivity determined by permeameter tests, the storativity could then be found. It showed no significant dependence on position but some dependence on period, with the larger storativities generally resulting for the longer period waves and the smaller storativities for shorter period waves. This particular aspect of the tidal response problem is discussed in more detail on pp. 14 to pp. 25 of this report.

One important result was found in the fact that for the unconfined

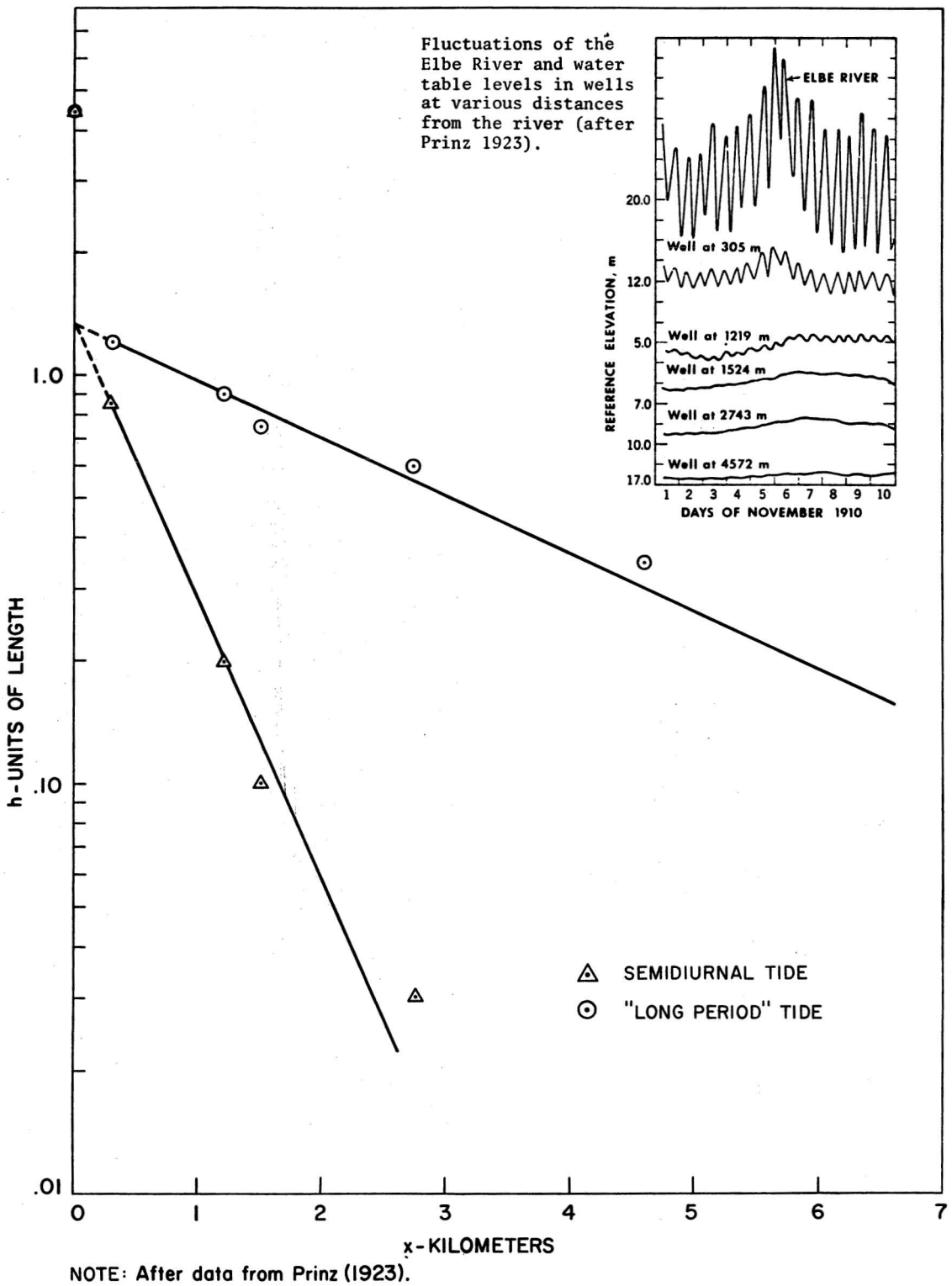

FIGURE 1. AMPLITUDE vs. DISTANCE FOR A FLUCTUATING WATER TABLE ADJACENT TO THE ELBE RIVER

aquifer model the storativities were only a small percent of the true porosity. When an average value of α based on the individual values computed for each of the several observation points was used as input, the mathematical and electric analog models produced results which were in generally good agreement with the hydraulic model.

Miller (1941) conducted a set of experiments similar to those described above which employed a Sacramento (Calif.) River sand placed in a tank 1 ft wide x 1.5 ft deep x 9.6 ft long. One test was conducted using a period of 10 mins. and a water depth of 1.105 ft. A 5-min. period was used for the remaining 5 tests while the water depth varied from 0.27 to 1.047 ft. The test results were presented in the form of graphs of amplitude and phase angle vs. position. Analysis of this data by Williams, Wada, and Wang (1970) produced results similar to those for the polyurethene foam. In particular, it indicated that the storativity varied from 1 to 5% of the true porosity, 0.345.

Williams and Liu (1971; 1973) developed mathematical and electric analog models of one-dimensional aquifers influenced by nonhomogeneity and by leakage. Two nonhomogeneous models were considered: the first was an aquifer of infinite length whose permeability (or thickness) changed discontinuously at a distance x=L from the coastline; and the second was an aquifer of finite length, L, whose permeability varied linearly with distance from the coast. The results for the discontinuous permeability model showed clearly the influence of the sudden change in conductivity as a discontinuity in the slope of the type-curves of amplitude and phase angle vs. position. The results of the linearly varying permeability model show type curves which differ in detail but are essentially similar to those curves for constant conductivity. In general, the amplitude curves (for the no-flow boundary condition) seem to flatten out more rapidly and indicate greater attenuation when the permeability increases rather than decreases with distance from the coast.

The leaky aquifer system consisted of two infinite aquifers separated by an aquitard. Results here indicated that a moderate amount of leakage would cause amplitudes and phase angles to vary by 100% or more from those where no leakage was present. Consequently, the presence of leakage in a real aquifer system would, at best, render tidal response data questionable.

One of the most thorough analyses of the aquifer in direct communication with the sea is given by van der Kamp (1973). Using a three-layered aquifer system as a model, he developed the following general solution to the basic

conservation of mass equation, i.e., the (linearized) Boussinesq equation:

$$h_j(x,z,t) = g_j(z)(A_1e^{px} + A_2e^{-px})\, e^{i\sigma t} \qquad (9)$$

Here, A_1 and A_2 are complex constants, σ is the tidal frequency, p is a complex number related to the hydrogeologic properties of the layers as well as to the tidal frequency and whose real and imaginary parts are the propagation parameters, and the function, $g_j(z)$, determines the potential distribution over the depth for the j-th layer. For a confined aquifer, i.e., the two outer layers are aquicludes and $g_2(z)$ is a constant; for an unconfined aquifer $g_2(z)$ is a quadratic equation. The above solution, which is generally not valid in the neighborhood of the coastal boundary, includes supplementary equations relating the hydrogeological properties to the propagation parameters for confined, semiconfined, and unconfined aquifers.[1] In the course of establishing these later relations, a set of criteria is derived for determining which of three aquifer types prevails.

The above relations are then tested with field data taken from a number of locations in the Netherlands and in Canada. Some of the data were analyzed to yield the pertinent hydrogeological properties of the layers which in turn were applied to the criteria for determining the aquifer type and to the equations for the propagation parameters. The tidal data provided an independent calculation of the propagation parameters. A comparison of the results of these calculations led the author to the general conclusions that the propagation parameters are more reliable when calculated from data other than tidal response data, that the criteria for determining the aquifer types are reasonably reliable,[2] and that vertical gradients were not as significant as initially anticipated.[3] The author also points out that for an

---

1. In the case of a thin aquifer with no vertical components to the potential gradient, the real and imaginary parts of the complex number $p = n + im$ reduce to $m = n = \sqrt{(S_2\sigma/T_2)} = \alpha_2$ as defined in eq. (5).
2. The criteria for a confined aquifer, i.e., $\sigma S_1(D_1/K_1') \gg 1$, appears to be particularly well corroborated by the field data. In this relation, the quantity, $D_1/K_1' = C_1$, is the resistivity to vertical flow of the upper layer and it has been assumed that the bottom layer is at least an aquitard if not an aquiclude.
3. The author points out that for the unconfined case, the influence of vertical gradients may be eliminated if all the observation points are placed at the same elevation within the aquifer.

unconfined aquifer the storativity at the water table appears to increase with the period of the flow, that there seems to be an "extra resistance to vertical flow near the water table," and that it is quite likely that these two phenomena are related.

Liu (1973) found that the shallow aquifer theory as expressed by equations (5a), (5b), and (5c) provided excellent predictions of the amplitudes for aquifers with depths as great as 22% of the penetration length and with the wave amplitude as much as 10% of the depth. Phase angle predictions were not as good, the observed values being 20% to 45% less than those predicted. The linear relation between phase angle and position was retained, however. Liu also observed that the storativity was dependent on the tidal frequency and the aquifer depth, except for the longest tidal period (9 sec) where it remained constant for the range at depths tested.

Recently, Philip (1973) has presented an analysis of the nonlinear diffusion equation by first applying Kirchhoff's transformation and then averaging the resulting equation in time. The second step applies a periodic time variation of the concentration at a boundary. The net result is a transformed problem which involves a solution to Laplace's equation and a transformed boundary condition which requires that the concentration be in excess of its equilibrium value at sufficiently large distances from the boundary. In terms of tidal diffusion this would require that the equilibrium level of the inland groundwater be above that of the mean sea level. This difference amounts of 23% of the tidal amplitude when the amplitude is equal to the thickness of the aquifer.

Aquifers in Indirect Communication with the Sea

The problem of indirect communication with the sea is complicated by the fact that while the aquifer extends continuously across the coastline, the region subjected to variations in loading terminates there.

Carr and van der Kamp (1969) argued that equation (5a) could be used provided that the amplitude $\zeta_o e^{-\alpha x}$ was replaced with $\zeta_o(t.e.)e^{-\alpha x}$ to account for the efficiency of the granular skeleton. The term, $(t.e.)e^{-\alpha x}$, is defined as the apparent tidal efficiency, $(t.e.)_{app}$. Carr and van der Kamp also observed that from equation (5a) the time lag required for any phase of the tide to penetrate a distance, x, into the aquifer is given by $t_{lag} = x\alpha/\sigma$. Thus, the expression for the apparent tidal efficiency can be written

$$(t.e.)_{app} = (t.e.)e^{-(\sigma t_{lag})} \tag{10}$$

Consequently, a measurement of $(t.e.)_{app}$ and t_{lag} together with a knowledge of the tidal frequency, σ, permits the calculation of t.e. and subsequently, S/b, the specific storativity, from equation (8), provided the porosity is known. As $\alpha = \sqrt{(S\sigma/2T)} = \sigma t_{lag}/X$ and S (or S/b) has been determined, then T (or K) can be found. This is the result of combining equation (8) with equation (5a) and is possible only for the case of indirect communication. Only α can be estimated for the case where the aquifer outcrops at the coastline. Carr and van der Kamp also point out that the observed lag times must be corrected for the response time of the well and that the observed tidal efficiency must also be corrected for a damping effect produced by the observation hole.

Application of the above theory to tidal data from a confined aquifer near Nine Mile Creek, P.E.I., Canada, produced results which were in reasonable agreement with those from a limited amount of pump test data. Also, their estimated tidal efficiencies and barometric efficiencies summed to .94 which agrees with equation (7) to within the expected error on the field measurements.

van der Kamp (1972) modified the basic differential equation of Boussinesq by accounting for the uniform, but time varying, tidal load on the subsea portion of the aquifer. This amounted to the inclusion of the term, $(t.e.)\partial h_s/\partial t$, in the differential equation to be satisfied in the subsea portion of the aquifer. The Boussinesq equation remained valid for that portion of the aquifer extending inland from the coastline. The solutions to these two equations were subjected to two boundary conditions which required the continuity of the piezometric head and the flux of water at the coastline. This resulted in two equations for the piezometric head, one applicable to the subsea portion of the aquifer and the other to the landward portion of the aquifer. Two significant features not present in the Boussinesq solution became evident. First, a seaward-propagating disturbance 180° out of phase with the landward propagating disturbance resulted from the solution to the modified Boussinesq equation and second, the expression for the amplitude of the disturbance in either portion of the aqui-

fer contained a factor of one-half.[1] For the landward portion of the aquifer the expression for the piezometric head is

$$h(x,t) = 1/2(t.e.)\zeta_o\, e^{-\alpha x}\sin(\alpha x^{-\sigma t}) \qquad (11)$$

van der Kamp also superposed these solutions in such a way as to represent the case of a confined aquifer overlain by a narrow rectilinear channel subjected to tidal fluctuations and a confined aquifer under an ocean traversed by a narrow strip of land. In the case of the narrow channel, the resulting equations predict a phase lead at the channel edge with respect to the tidal change which gradually decreases and becomes a lag as the channel width increases beyond $3/\alpha$.

To support the two results of his analysis, van der Kamp points out that equation (7) may be rewritten as

$$b.e. + (t.e.)_0 = 1\text{-}1/2(t.e.) \qquad (12)$$

where $(t.e.)_0=1/2(t.e.)$ is the tidal efficiency at the coastline. Thus, the barometric efficiency and the tidal efficiency observed at the coastline should sum to a number less than unity for aquifers extending under the sea. Data from a semiconfined sandstone aquifer at York Point, P.E.I., Canada, and from a confined at Cap-Pelé, N.B., Canada, give values of .79 and .71, respectively, for the sum.

De Cazenove (1971) analyzed aquifers communicating both directly and indirectly with the sea. His analyses are quite extensive and include a variety of boundary conditions as well as the case where leakage takes place at some point in the subsea portion of the aquifer. In particular, his analyses include the same problem[2] as discussed by van der Kamp and his results for the amplitude include the factor of one-half. He also analyzes the case where the landward portion of the aquifer is of finite extent. The expression for h in the finite portion of the aquifer is

$$h = \frac{(t.e.)\zeta_o}{2}\{e^{-\alpha x}\sin(\sigma t-\alpha x) + e^{\alpha(x-2D)}\sin[\sigma t+\alpha(x-2D)]\} \qquad (13)$$

1. This is the result of the continuity condition at the coastline which requires one-half the disturbance to propagate seaward and the other half to propagate landward with a 180° phase difference between the two.
2. This case was apparently first solved by J. Brillant in 1965. See De Cazenove (1971).

where D is the distance which the aquifer extends inland from the coastline.

Dale (1974) has developed a digital modeling technique based upon the finite difference form of the basic differential equations of flow in a shallow aquifer. He identified twelve different aquifer types on the basis of a boundary and loading conditions and computed type-curves, i.e., the variation of amplitude and phase angle with respect to distance from the coastline, for each type. The modeling technique was verified by the comparison with closed form solutions of Williams, Wada, and Wang (1970) for both the one-dimensional and the circular island aquifers.

In addition, field data from four local aquifers were matched to type-curves with varying degrees of success. The P_1 plus the K_1 and the M_2 were the tidal constituents used in matching the type-curves. The harmonic analysis used was based on 28-day records and followed the technique of Doodson (1922). In particular, the type-curve match for the shallow (unconfined) Ewa Beach limestone aquifer resulted in K/S= 2 to 4×10^7 sq fpd. For the confined basaltic aquifer underlying Pearl Harbor, the type-curve match is made for an aquifer which suddenly becomes unconfined in the vicinity of its interior boundary. The digital model simulates this condition by allowing the storativity to increase to unity over a relatively short distance, which effectively imposes a constant head boundary condition or a "standpipe condition" at the interior boundary. The type-curves show a phase lead with respect to the tide in this region which is confirmed by field observations from wells located near the end of the confining layer.[1]

It should be noted that the above modeling technique is applied to unconfined aquifers by taking sufficiently large values of the storativity. Also, all of the above models are based on a one-dimensional flow in that only one space variable is considered.

Lam (1971) has studied the tidal diffusion problem of an atoll. He developed five models which represent various combinations of boundary conditions for the atoll and the enclosed lagoon. The output of the models was compared for several tidal components (viz., M_2, S_2, N_2, K_1, and O_1) with those measured in the lagoon and at eight observation wells on Swains Island, an atoll in the Tokelau or Union Islands group.[2]

1. This observation is also consistent with van der Kamp's (1972) analytical result for a confined aquifer overlain by a narrow channel.
2. The Tokelau Islands group is approximately 2000 miles south and slightly west of the island of Oahu, Hawaii.

One interesting aspect of this study was the computation of the power spectrum for the tide at each observation point. This analysis indicated maximum power for the semidiurnal tide and a lesser amount for the diurnal component, but did not distinguish between the several semidiurnal or diurnal constituents.

His results indicated that the permeability of the atoll varied from 4.4×10^{-6} sq cm to 14.1×10^{-6} sq cm with the larger values resulting from the phase lag measurements and the smaller ones from the amplitude measurements. Considering all five models, extreme values of permeability differ by three orders of magnitude. The porosity of the reef material, based on core samples, varied from .55 to .77.

AN EXPERIMENTAL STUDY OF THE EFFECTIVE POROSITY FOR AN OSCILLATING WATER TABLE

Introduction

The results of the Williams, Wada, and Wang (1970) study indicate some dependence of the storativity on time for both the confined and unconfined cases. Also, Bear, Zaslavsky, and Irmay (1968) point out that in the case of the unconfined aquifer, the amount of water removed per unit of drawdown per unit of horizontal area is the instantaneous dewatering coefficient, m, which after sufficient time may approach the effective porosity which is approximately equal to the specific yield. The basic equation which relates the dewatering coefficient, m, to the instantaneous dewatering rate, r, and the drawdown, ds, which occurs in time, dt, is

$$mds = rdt \, . \tag{14}$$

Experimental Considerations

In order to obtain more information on this phenomenon, several sets of experiments were preformed. The first set of experiments involved the measurement of a volume of water drained from a column of porous media together with the corresponding head drop observed in a piezometer tube attached to the column. This was accomplished by collecting water for a given period and noting the elevation of the piezometric head at the end of the period, at which time the partially filled collection container was replaced by an empty one. With a little care, this operation could be carried out without any

spillage. Hence, the cumulative volume of drained water together with the associated elevation of the piezometric head was obtained.[1] The fluid volume was divided by the area of the column and plotted as a function of s, the piezometric head drop. From equation (14), it is clear that the slope of this curve at any point is the instantaneous dewatering coefficient, m. Two different materials were used: the first was Ottawa sand and the second was polyurethene foam used by Williams, Wada, and Wang (1970). The plotted results are shown in Figure 3. Figure 4 shows a dimensionless plot of the same quantities for the Ottawa sand where the values of $\forall/A$ and s at the inflection point of the curve have been used to nondimensionalize the ordinate and abscissa, respectively. A schematic representation of the experimental setup for both the foam and the sand is included in Figure 2a. Figure 5 shows the grain size distribution for the Ottawa sand as well as the Sacramento River (California) sand used by Miller (1941) in his experiments on the tidal response of groundwater aquifers.

The second set of experiments was designed to account for the periodic nature of the time variation characteristic of tidal response phenomenon. In this instance, the column was connected to a cylinder of water by a short piece of flexible tubing. The cylinder of water was then placed in rectilinear harmonic motion along its axis. Figure 2b shows a schematic representation of this arrangement. As seen from Figure 2b, the volume of water moving out of, or into, the aquifer column is $s_r A_r$ and the volume of media which is apparently drained or filled is $s_a A_a$. Hence, the effective porosity $\varepsilon' = s_r A_r / s_a A_a$ where A_r should be corrected for the area occupied by the two resistance probes used for recording the water surface elevations in the reservoir cylinder. Since these probes are secured to the reservoir cylinder, they record the motion of the water relative to the cylinder and s_r may be read directly from the trace on the chart paper. The head, s_a, was recorded by means of a stationary pressure transducer connected to the aquifer column. Calibration of the resistance probes was accomplished by clamping off the flexible tubing between the aquifer column and the reservoir cylinder and then changing the water surface elevation in the reservoir by a given amount and noting the corresponding change on the recorder chart. With the flexible

1. The ratio of the diameter of the piezometer tube to that of the column was less than .05. This results in a contribution to the collected water volume from the piezometer tube of less than one percent. Hence, the measured volumes were not corrected for the small error.

L = Total sample length

S = Piezometric head drop

Ψ = Volume of water collected under head drop, s

A = Area of Column

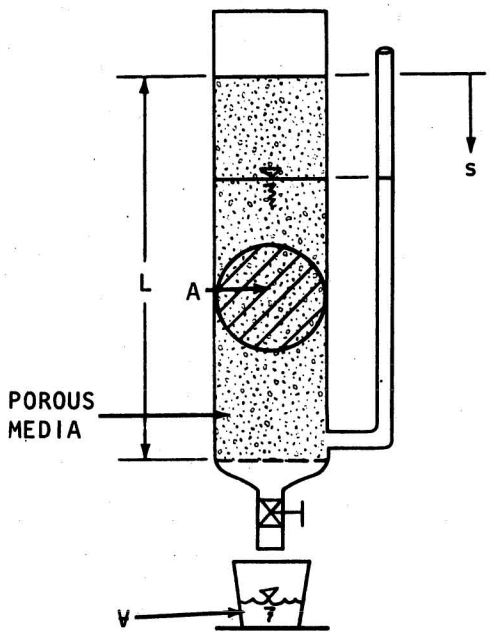

FIGURE 2a. SCHEMATIC DIAGRAM OF EXPERIMENTAL SETUP FOR FOAM AND SAND TO DETERMINE THE DEWATERING COEFFICIENT, m

ζ_o = Amplitude of water column oscillation

s_r = Distance water level deflects in water column relative to equilibrium level - measured directly from recorder chart

s_a = Deflection of phreatic surface in aquifer column - measured directly from recorder chart

A_r = Area of water column corrected for area of resistance probes

A_a = Area of aquifer column

L_a = Total length of aquifer column

$\bar{z}$ = Depth to equilibrium level

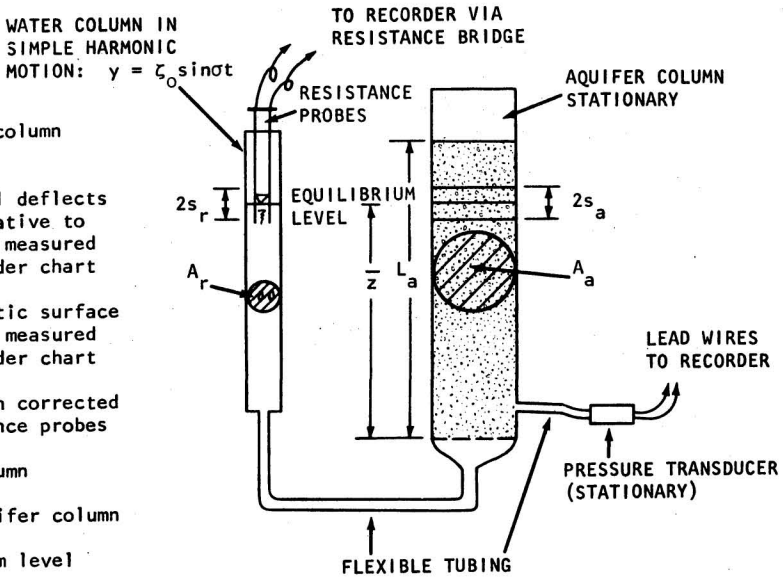

FIGURE 2b. SCHEMATIC DIAGRAM OF EXPERIMENTAL SETUP TO DETERMINE THE EFFECTIVE POROSITY, ε', UNDER A PERIODIC FLUCTUATION OF THE PIEZOMETRIC HEAD

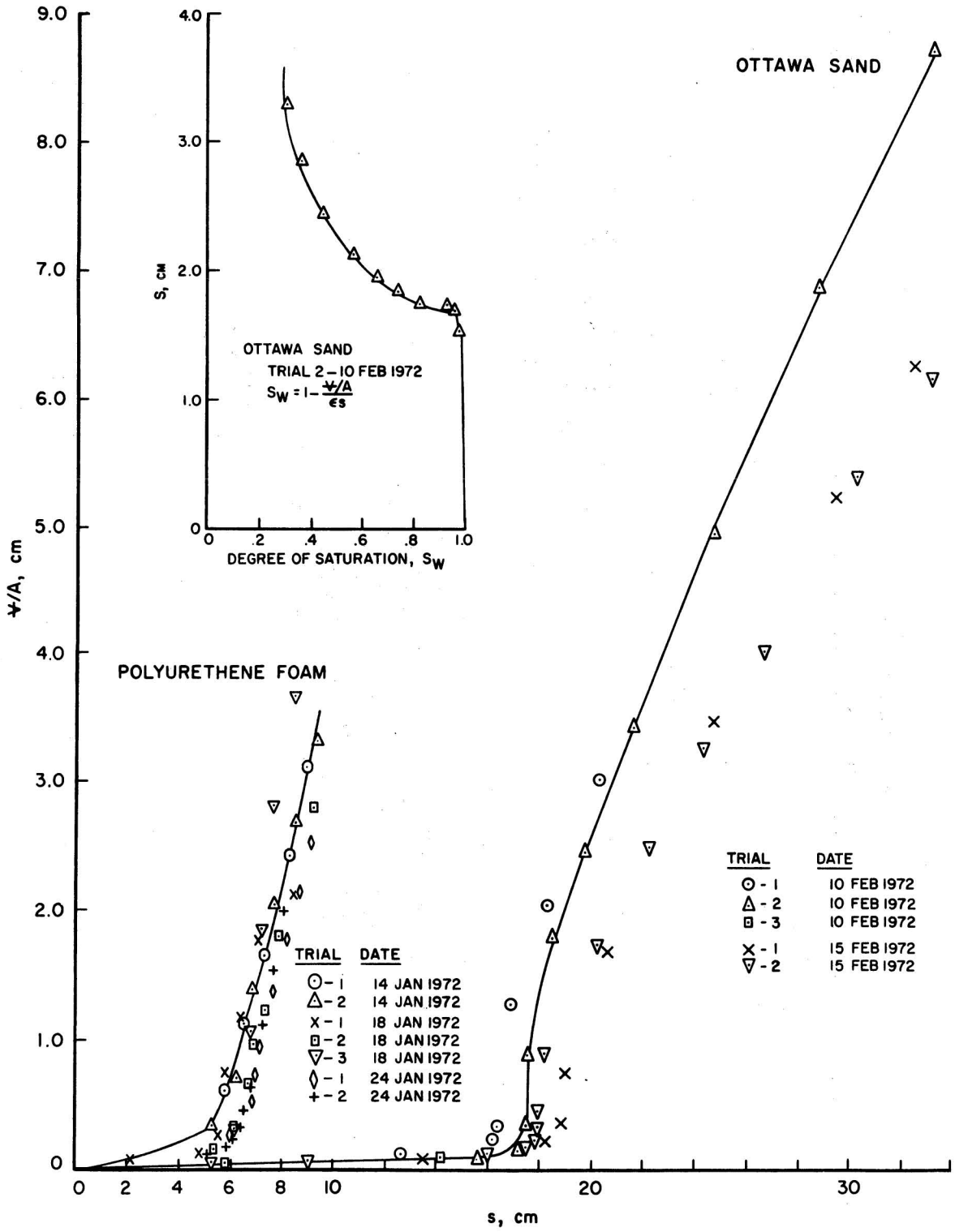

FIGURE 3. PLOT OF WATER VOLUME PER UNIT AREA OF COLUMN VS. DRAWDOWN FOR POLYURETHANE FOAM AND OTTAWA SAND

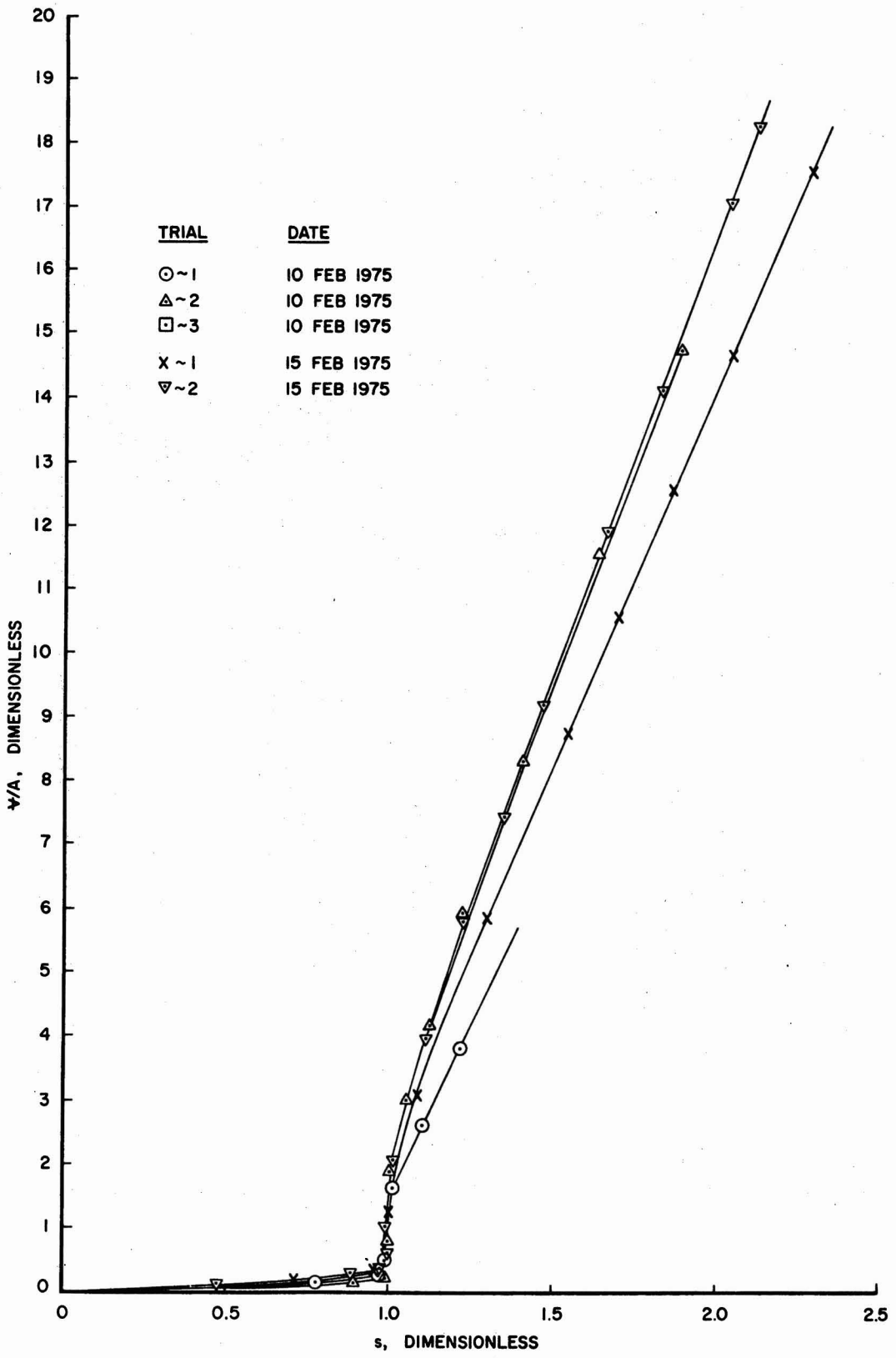

FIGURE 4. DIMENSIONLESS PLOT OF WATER VOLUME PER UNIT AREA OF COLUMN, Ψ/A, vs. DRAWDOWN, s, FOR OTTAWA SAND

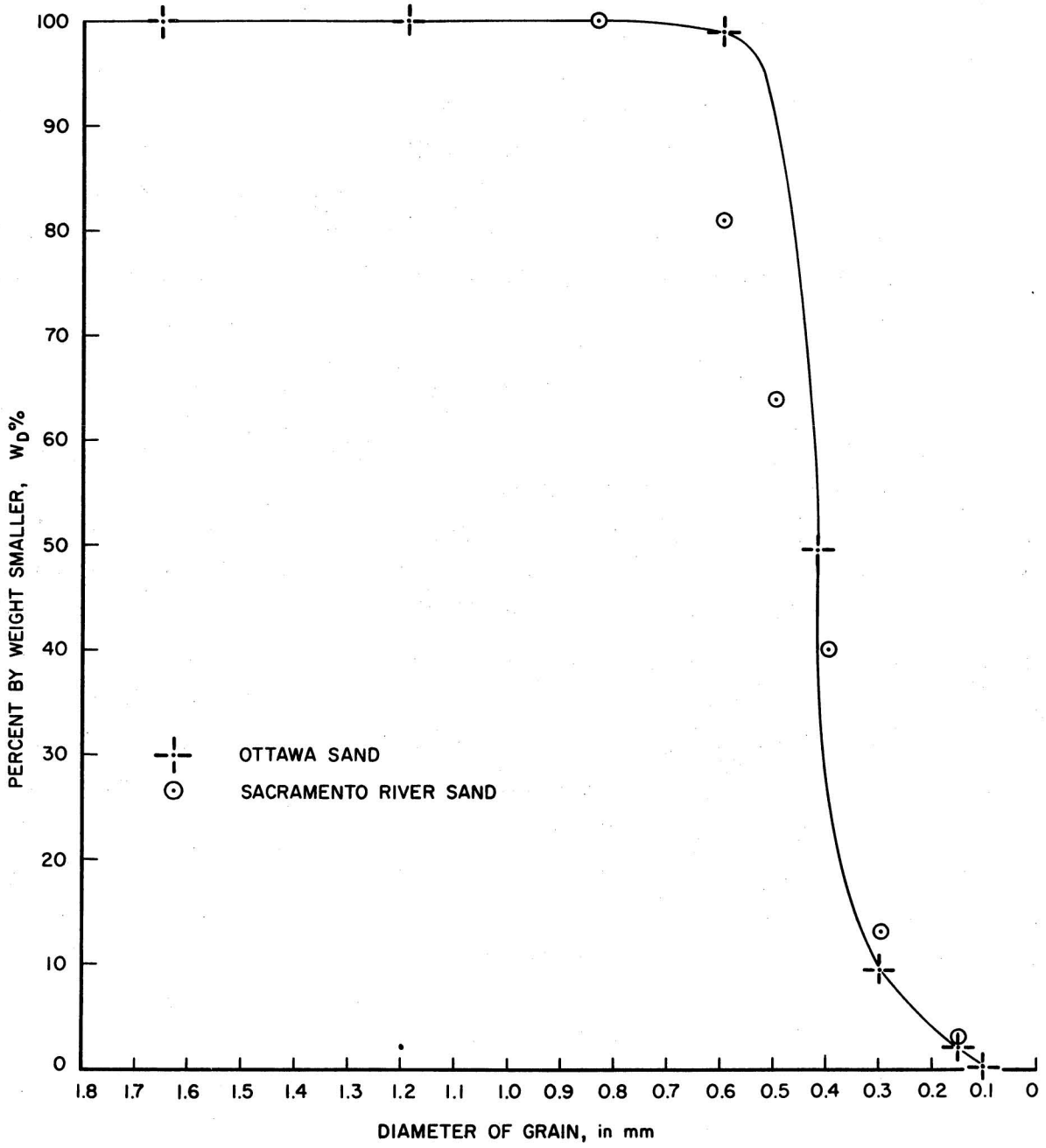

FIGURE 5. GRAIN SIZE DISTRIBUTION FOR OTTAWA SAND AND SACRAMENTO RIVER (CALIFORNIA) SAND

tubing still clamped off, the pressure transducer was calibrated by raising or lowering the entire aquifer column a given amount and observing the corresponding change on the recorder chart. Both the polyurethene foam and the Ottawa sand were tested.

For both materials, several different column lengths were used, and several water depths, $\bar{z}$, were used with each column length. Tests were run at each water depth using three different amplitudes, ζ_0, for the harmonic oscillation of the reservoir cylinder. Data were recorded for periods of oscillation, t_o, varying from 2 to 30 sec at each amplitude. The results of these tests and the values of the pertinent parameters involved are presented in Figures 6, 7, and 8.

Experimental Results

From the results of the first series of experiments shown in Figures 3 and 4, it is clear that the instantaneous dewatering coefficient is very small until the phreatic surface has dropped 12 to 18 cm in the sand column and about 5 cm in the polyurethene foam column, at which time it increases sharply, i.e., the curve takes a nearly vertical slope. The slope then decreases gradually to what should be close to the specific yield. The sharp increase in m is particularly evident in the dimensionless plot of Figure 4 and is the point at which the capillary forces can no longer support the volume of water retained in the pore spaces. The curve slopes for the foam and the sand (Trials 1 and 2, 15 February 1972) approach values of .8 and .34, respectively. As the true porosity of the foam is .97[1] and that of the sand was calculated at .382, these values for the slopes are reasonable estimates of the specific yield for the two materials.

It is interesting to note that the results shown in Figures 3 and 4 can be expressed as a plot of s vs. $S_w=1-(\Psi/A)/(\varepsilon s)$ where S_w is the "degree of saturation" of the drained portion of the column. This produces the typical capillary head-saturation curve shown in the insert of Figure 3. It is seen that the head drop which corresponds to the maximum value of $m=d(\Psi/A)/ds$ is the "bubbling pressure" or the "air entry value."

From the results of the second set of experiments, it is apparent that

1. Other pertinent properties of the foam as determined by Williams, Wada, and Wang (1970) are: Young's modulus, E = 13.6 psi
Hydraulic conductivity, K_{avg} = .17 fps
Specific storativity, S_s = .032 ft^{-1}

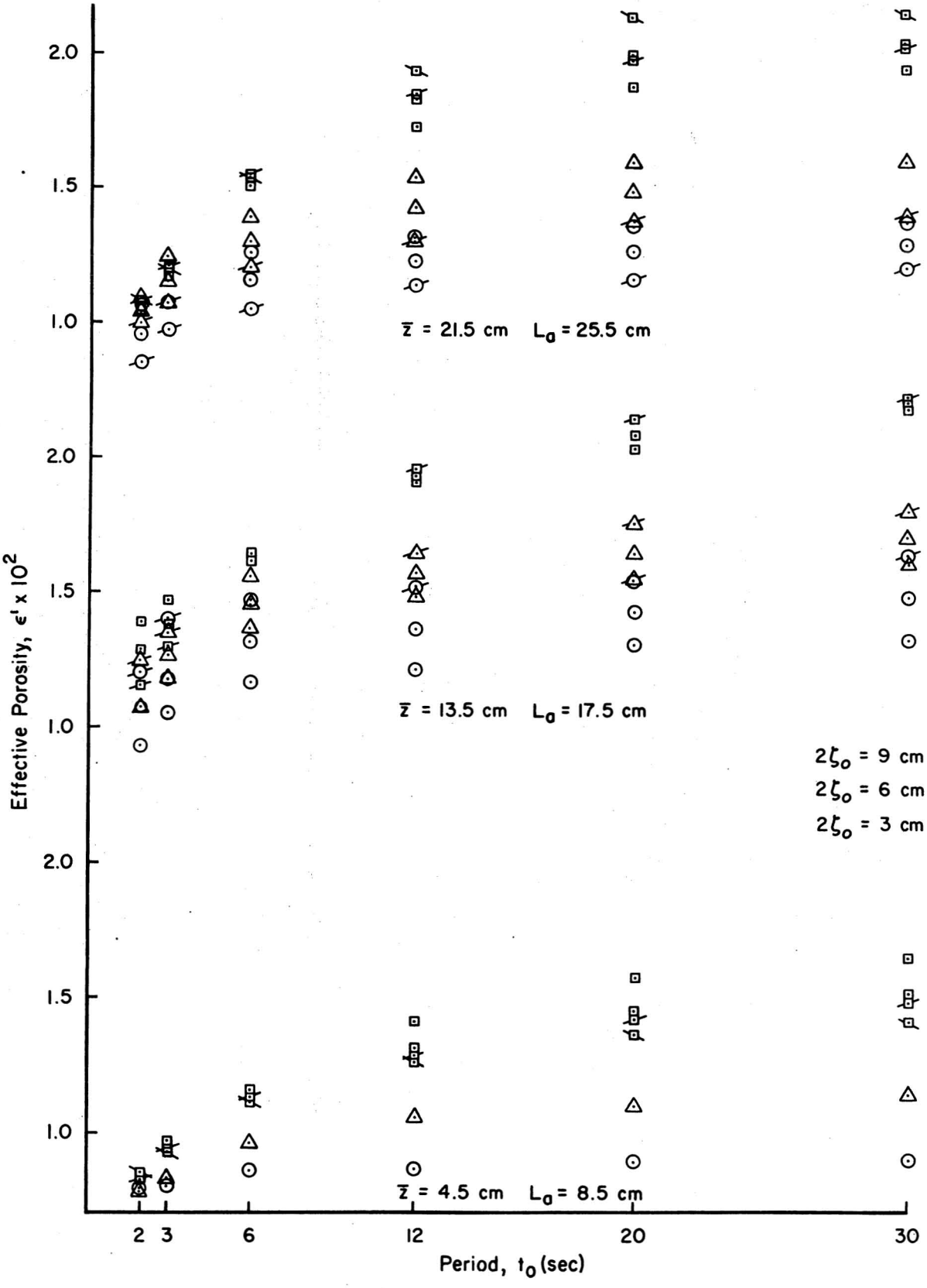

FIGURE 6. PLOT OF EFFECTIVE POROSITY, ε', vs. PERIOD, t_o, FOR POLYURETHENE FOAM

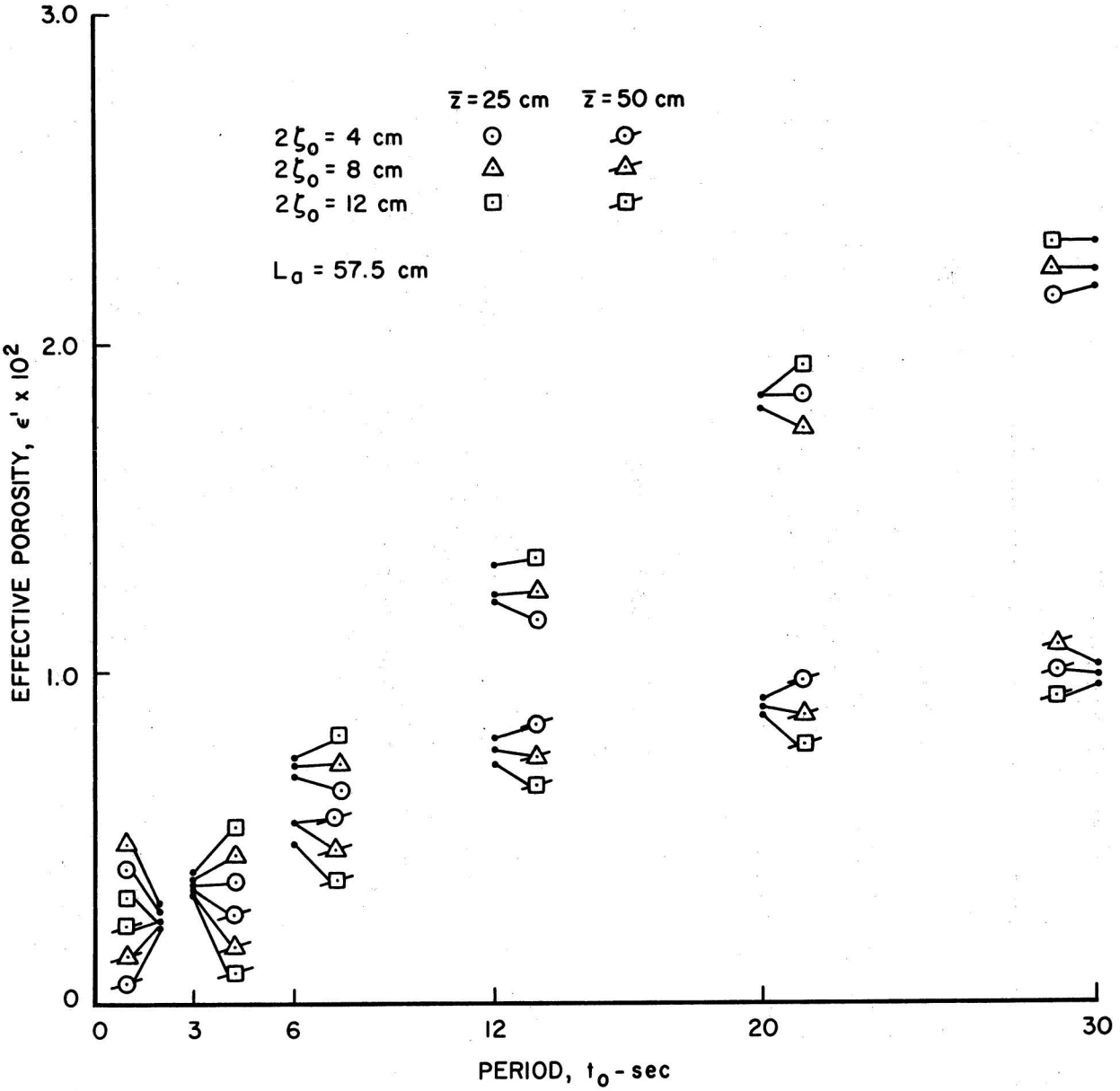

FIGURE 7. PLOT OF EFFECTIVE POROSITY, ε', vs. PERIOD, t_o, FOR OTTAWA SAND, L_a = 57.5 cm

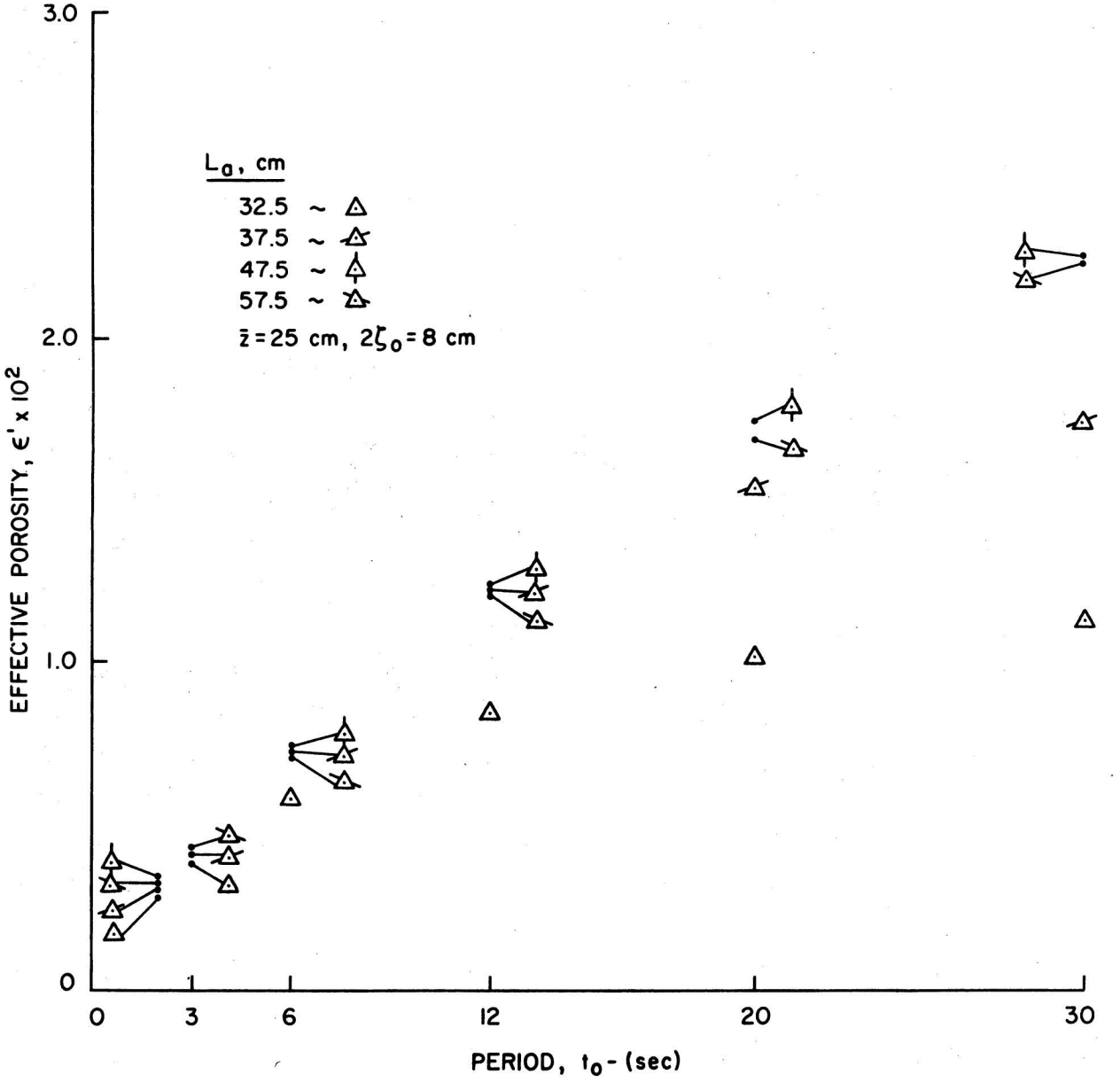

FIGURE 8. PLOT OF EFFECTIVE POROSITY, ε', vs. PERIOD, t_o, FOR OTTAWA SAND, $\bar{Z}$ = 25 cm

the effective porosity in both materials depends upon the period of oscillation of the piezometric surface. The effective porosity of the foam shows a strong dependence on the amplitude of the oscillation and that of the sand shows very little, if any. The tests on the sand do show, however, a strong dependence of ε' on the depth of media above the phreatic surface. In the tests on the foam, this distance was held at 4 cm and no such variations were possible. Two additional facts are clear. The magnitude of ε' is on the order of .01 to .08 for both the foam and the sand, and the slope of the ε' vs. t_o curve is close to and/or approaching zero for periods greater than 30 seconds.

Summary

The effective porosity depends primarily on the amplitude and period of the oscillation in the piezometric head and on the depth of the material above the phreatic surface. For amplitudes of oscillation smaller than the critical distance at which the weight of suspended water overcomes the capillary forces supporting it, relatively little volume will be vacated or filled during the periodic cycle, regardless of how long the period of fluctuation. This is apparent in the tests on the foam using the smallest amplitude of 1.5 cm. However, as this amplitude increases and approaches the critical value, ε' will increase and show a stronger dependence on the period, as it does for the foam when the amplitudes are increased to 3 and 4.5 cm, respectively. Note that the critical distance for the foam from Figure 3 is about 5 cm, while that for the Ottawa sand varies from 12 to 18 cm. Consequently, the results from the tests on the sand showed little dependence on amplitude as 6 cm was the maximum amplitude tested.

The dependence of ε' on the depth of the porous media above the phreatic surface seems to diminish as this distance increases. For example, a significant difference is apparent between the test results employing a total column length of 32.5 cm and 37.5 cm with an equilibrium water depth of 25 cm in both cases. However, an increase in column length to 47.5 cm produces a much smaller change in the ε' vs. t_o curve and a further increase to a column length of 57.5 cm produces no additional change. This is most likely because the capillary fringe region does not get a chance to develop completely when there is not a sufficient depth of media above the phreatic surface. The critical depth of material should be the same as the critical distance

through which the head must drop to produce the sharp increase in the instantaneous dewatering coefficient as discussed above. For the sand this amounts to an average of 15 cm. Adding 15 cm to the water depth of 25 cm gives 40 cm of approximately the total column length which, if exceeded, will produce no change in the ε' vs. t_o curves of Figure 8.

Finally, the very small values of ε', i.e., .005 to .025, resulting from the test data confirms the conclusion of Williams, Wada, and Wang (1970) that only 1 or 2% of the available porosity is utilized as storage in polyurethene foam and Sacramento is utilized as storage in polyurethene foam and Sacramento (Calif.) River sand.[1] Furthermore, it is a reasonable speculation that this conclusion may be extended to prototype conditions in view of the results indicating that ε' is weakly dependent or possibly independent of time for periods in excess of several minutes. van der Kamp points out that on the basis of field measurements, the specific yield of unconfined aquifers can be of the order of 10^{-2}.* It should be observed that the fluctuation in the piezometric head will most likely never exceed the height of capillary rise in a prototype situation, except possibly in a region extremely close to the coastline. Hence, the storativity will be determined essentially by the smallest value of the instantaneous dewatering coefficient, i.e., by the smallest or initial slope of the $\forall/A$ vs. s curve.

EWA BEACH SHALLOW LIMESTONE AQUIFER SIMULATION

Description of the Aquifer, Wells, and Field Data

THE AQUIFER. The Ewa Beach aquifer is located on the leeward coast of the island of Oahu in the Hawaiian Islands chain. The aquifer is composed of coral and limestone and varies in thickness from approximately 200 ft at the seaward end to approximately 100 ft at the landward boundary which is assumed to be impermeable to water flow. The areal extent of the landward portion of the aquifer is bounded by the coastline from Brown's Camp to the Salt Evaporators adjacent to the West Loch of Pearl Harbor. The interior boundary is taken as the old rail line which extended from Brown's Camp along the Barbers Point Naval Air Station to the Salt Evaporators. These

1. The Williams, Wada, and Wang (1970) analysis of Miller's (1941) data shows $.009 \leq \varepsilon'/\varepsilon \leq .048$ and $\overline{\varepsilon'/\varepsilon} = .026$ for the 6 tests conducted. For the longest period tested, (i.e., t_o=10 min.) $\varepsilon'/\varepsilon = .020$.

* G. van der Kamp 1973: personal communication.

boundaries encompass an area of approximately 20 sq miles. A map of this area is shown in Figure 9. The aquifer is unconfined, and the lower boundary consists of highly impermeable marine mud.

THE WELLS. Two wells for which tidal data were available are located in the area. They were constructed by the Oahu Sugar Company for irrigation purposes and are designated as Dug Wells Nos. 40 and 41.[1] The locations of these wells are indicated on the map shown in Figure 9 and they may be seen in the aerial photograph presented in Figure 10. The significant feature about these wells is that they are located in old coral excavation pits and consist of long channels, hollowed out of the ground with a bulldozer, extending only 6 to 10 ft below the water table. This permits the lower density fresh water to be skimmed off the top of the aquifer by pumping from a point along the channel.

FIELD DATA: ACQUISITION AND ANALYSIS. The field data for the wells were obtained from the files of the district office of the U.S. Geological Survey, Water Resources Division. Data consisted of time-elevation histories for the water surface in Dug Wells Nos. 40 and 41, recorded over a period of 2 weeks from 26 August 1965 to 8 September 1965. During this period, the pumps in both wells were turned on for short periods on several occasions in order to record the drawdown in the wells. Unfortunately, the periods of pumping were so short that essentially only water stored in the channels was extracted during the test. Hence, the drawdown data do not reflect the aquifer properties. Also, the rates of drawdown and recovery in both wells were so rapid with respect to the recorder chart speed that these events appear as essentially straight vertical lines on the chart. Consequently, an analysis of the pumping test data was not feasible. The portions of the time history recorded during pumping and recovery were removed from the record, leaving only the tidal response. This modified time history is presented in Figure 11.

The tide data recorded on the NOAA gage located in Honolulu Harbor[2] was analyzed and used since no tide records were available for the Ewa Beach region. According to Dale (1974), there is no difference in the Pearl Har-

1. According to a recently adopted identification system established by the U.S. Geological Survey, Dug Wells Nos. 40 and 41 are now identified as wells 1902-01 and 1900-13, respectively.
2. The National Oceanic and Atmospheric Administration maintains a Fisher and Porter recording tide gage at Pier 4, Honolulu Harbor.

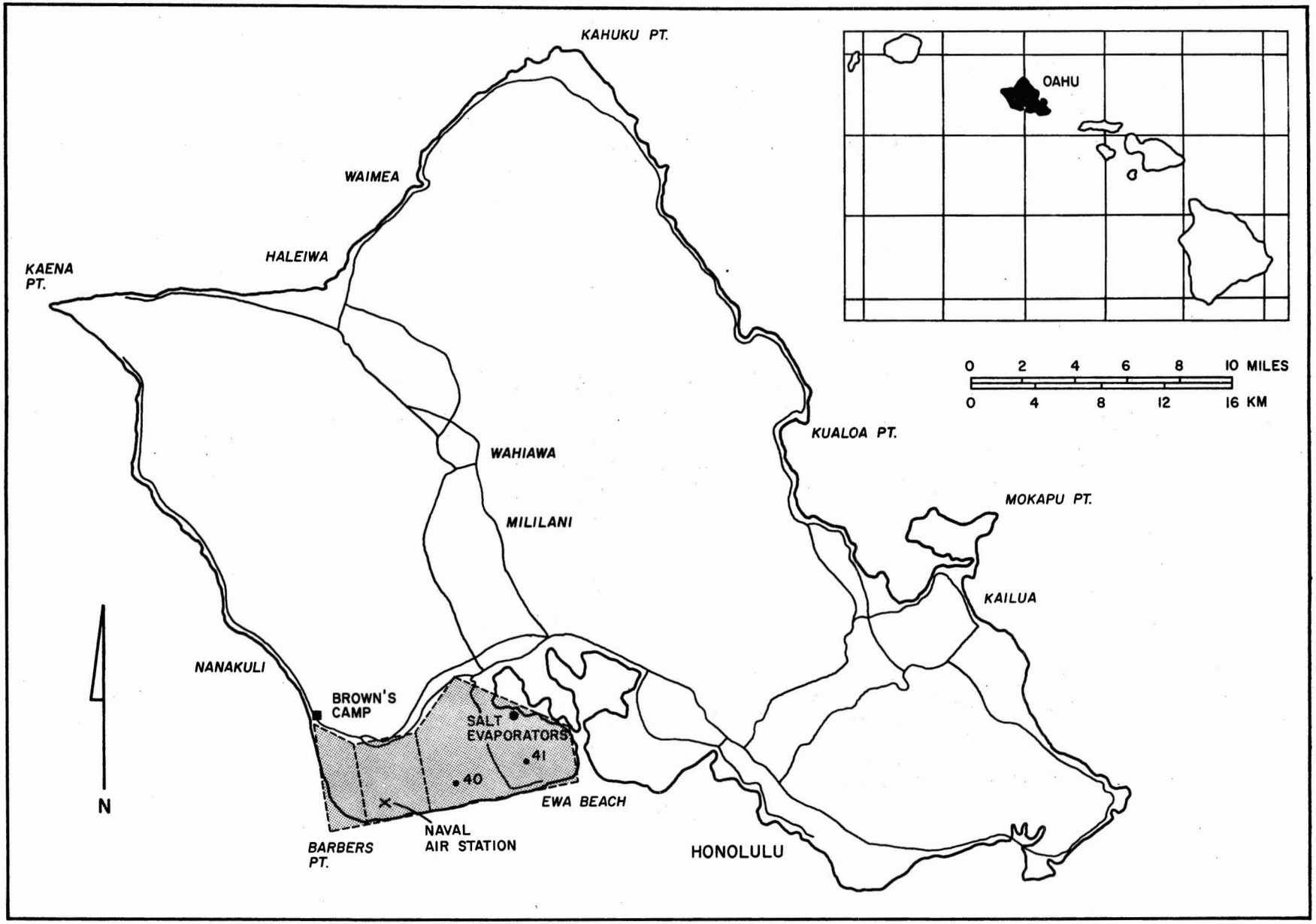

FIGURE 9. LOCATION OF CORAL LIMESTONE AT EWA BEACH, OAHU

SOURCE: BASE MAP FROM R.M. TOWILL CORP. (1971); SCALE: 1 in. = 1600 ft.

FIGURE 10. AERIAL PHOTO OF REGION AROUND DUG WELLS NO. 40 AND NO. 41

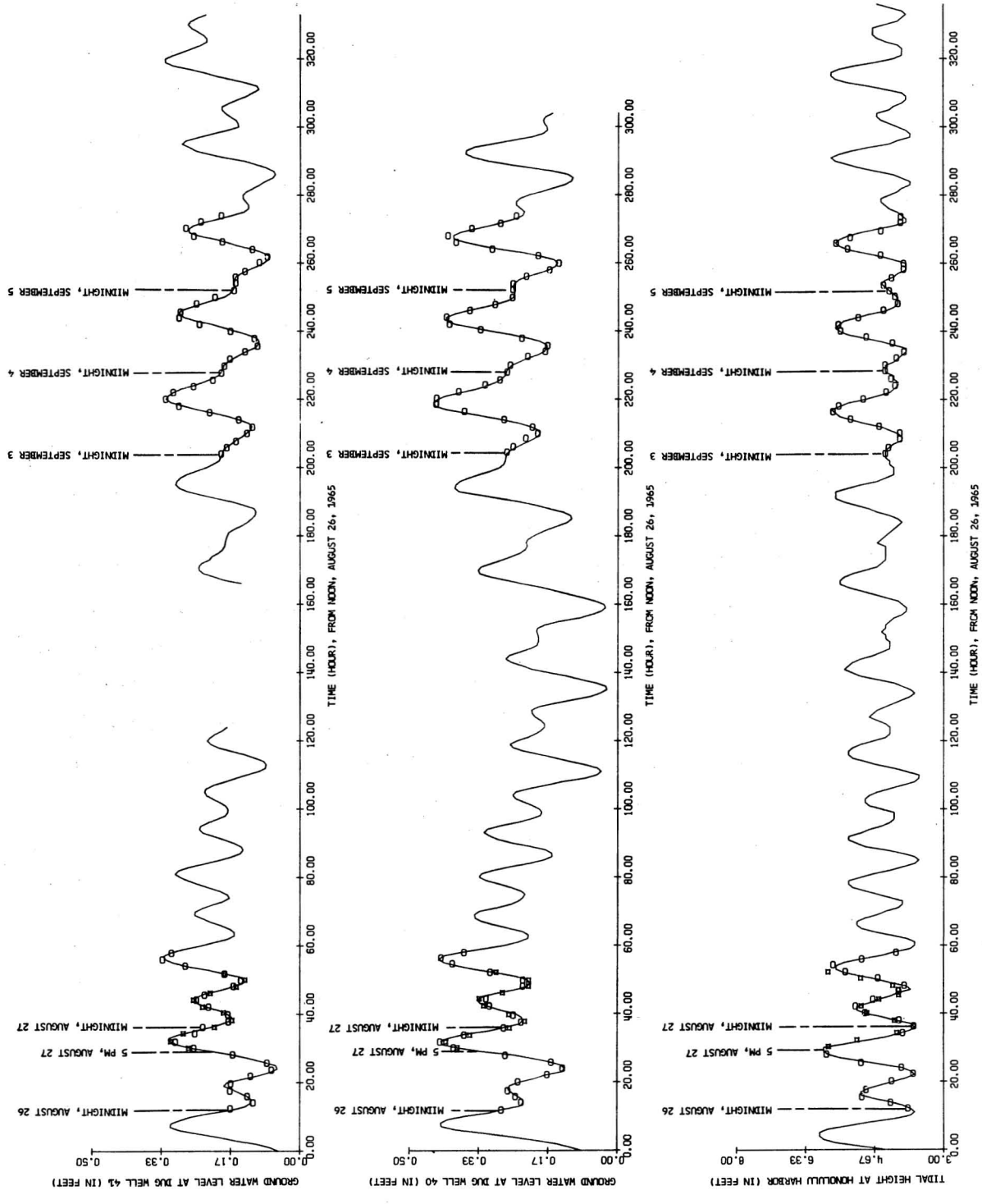

FIGURE 11. WATER SURFACE-TIME HISTORY FOR DUG WELLS NO. 40 AND NO. 41 AND THE TIDE FOR HONOLULU HARBOR, 26 AUGUST 1965 TO 9 SEPTEMBER 1965

bor tide and that at Honolulu Harbor except that the former leads the latter by about a quarter of an hour. Hence, the Honolulu Harbor tide was considered a good representation of the actual tide along the Ewa Beach coast. The data were obtained from the Tides Branch, Oceanographic Division, National Ocean Survey, Rockville, Maryland and consisted of water level elevations, referenced 3.66 ft below MLLW, at hourly intervals for the months of August and September 1965. Figure 11 also shows a plot of this data for the period 26 August to 7 September 1965.

The analysis applied to the tidal records should resolve the basic harmonic constituents present. However, the particular technique employed will be determined essentially by the records themselves. From Figure 11, it is evident that for Dug Well No. 41 a 2-day segment of the record is missing. In addition, there appears to be some drift of the recorder used on Dug Well No. 40 over the period 29 August to 1 September as well as on 27 August, where the records from both wells show an almost discontinuous shift upwards. Tidal constituents of longer periods possibly corresponding to the fortnightly or monthly variations also seem to be present.

From a consideration of these limitations, it was decided to analyze 24-hr segments of the record where each segment was assumed to consist of only the diurnal (24 hr) and semidiurnal (12 hr) components. The particular technique selected was the periodogram analysis, used by Williams (1965), which involves the fitting of an nth order trigonometric polynomial to the 24-hr segments of the record. In general, if the record is composed of a set of harmonics, then it may be represented by

$$\zeta(t) = \frac{a_0}{2} + \sum_{p=1}^{n} (a_p \cos p\theta + b_p \sin p\theta) \tag{15a}$$

where

$$a_p = \frac{2}{2n+1} \sum_{k=0}^{2n} y_k \cos kp\alpha \; ; \; b_p = \frac{2}{2n+1} \sum_{k=0}^{2n} y_k \sin kp\alpha \tag{15b}$$

and $\alpha = 2\pi/(2n+1)$. The measurement of the ordinates, y_k, at 2n+1 evenly spaced points along the time axis then provides 2n+1 linear equations from which the 2n+1 unknowns a_0, $a_1, \ldots, a_n$, $b_1, \ldots, b_n$ may be found.[1] The ordi-

1. Equations 15a and 15b for the periodogram analysis are a special case of the more general "least squares" technique where the number of equations may exceed the number of unknowns. In this case, the 2n+1 is replaced by N and $\alpha = 2\pi/N$, where $N > 2p$. See Whittaker and Robinson (1967).

nates, in this instance, were measured from a baseline which was constructed parallel to what appeared to be the longer period variations in the record. This procedure should minimize or, at best, eliminate the influence of such variations from the record.

Since the wave form was assumed to consist of only the diurnal and semidiurnal components, n = 2 in equation (15b), and the a_p and b_p were calculated using five evenly-spaced ordinates scaled off the records shown in Figure 11. The resulting trigonometric polynomials given by equation (15a) are also plotted in Figure 11 on their corresponding segments of record. The amplitudes and the phase angles calculated from the relations $(a_p^2+b_p^2)^{\frac{1}{2}}$ and $\tan^{-1}(b_p/a_p)$ respectively, for both the diurnal and semidiurnal components are presented in Table 2.

The power spectrums for both the Honolulu Harbor and Dug Well No. 40 records were computed in order to investigate the lumping together of the diurnal constituents and the semidiurnal constituents into a fundamental (24-hr) period and a second harmonic (12-hr) period, respectively. The technique used was that of Blackman and Tukey (1959). The power spectrum for Dug Well No. 40 is limited necessarily by its length of 306 hr or 12.75 days while that of Honolulu Harbor is based on 1464 hr or the entire 61 days of August to September 1965. Even though the time lag should not exceed approximately one-tenth the length of the record, lags up to 60 hr were used for the Dug Well No. 40 spectrum and up to 120 hr for that of Honolulu Harbor. The results of the spectral analysis are presented in the form of graphs of spectral density vs. frequency, and autocovariance vs. time lag. These graphs are shown in Figures 12 and 13 for Honolulu Harbor and Dug Well No. 40, respectively.

The power associated with the 24-hr segments of record were estimated from the relation $1/2\sum_{p=1}^{n}(a_p^2+b_p^2)$. These estimates of the power together with those from the spectral analysis are presented in Table 3.[1]

Description of the Electric Analog Model and Model Data

ELECTRIC ANALOG MODEL. The model was laid out on U.S.G.S. maps of the Ewa Beach and Puuloa regions of Oahu. Since the map scale was 1 in. = 2000 ft, a grid spacing of a = 2000 ft was selected. This left a one-inch spac-

1. The power in the spectrum is the area under the spectral density curve and is equal to the autocovariance at zero lag.

TABLE 2. RESULTS OF HARMONIC ANALYSIS

		SEGMENT OF RECORD ANALYZED							
		8/27-28/65	8/27/65	8/28/65	9/04/65	9/05/65	9/06/65	AVG.*	6/22 to 7/22/65†
HONOLULU HARBOR	a_D, ft	.4747	.4620	.2688	.6441	.5753	.5606	.5022	.63
	a_S, ft	.7632	.8456	.7903	.4199	.4367	.5223	.6030	.58
	θ_D, deg	-14.54	225.86	241.08	193.32	203.58	211.47	215.06	235.1
	θ_S, deg	7.60	146.26	168.35	11.96	32.76	57.30	83.33	167.4
DUG WELL NO. 40	a_D, ft	.0404	.1001	.0498	.1104	.0978	.0998	.0916	.15
	a_S, ft	.0798	.0750	.0744	.0416	.0508	.0594	.0602	.04
	θ_D, deg	52.77	321.23	300.13	242.34	249.74	255.06	273.70	293.5
	θ_S, deg	74.37	214.25	226.66	62.63	71.58	82.05	131.43	224.1
DUG WELL NO. 41	a_D, ft	.0330	.0670	.0451	.0904	.0784	.0732	.0708	.08
	a_S, ft	.0660	.0688	.0699	.0320	.0342	.0394	.0489	.04
	θ_D, deg	75.53	314.58	323.41	260.00	277.72	287.30	292.60	324.5
	θ_S, deg	88.10	227.94	248.29	103.15	119.22	146.72	169.06	275.7

* THE AVERAGES RECORDED DO NOT INCLUDE THE RESULTS FOR 27-28 AUGUST 1965.
† FOR ENTRIES HERE a_D IS BASED ONLY ON C_{28} OR THE P_1 PLUS THE K_1 TIDAL COMPONENT AND a_S IS BASED ONLY ON C_{54} OR THE M_2 TIDAL COMPONENT FOR THE INDICATED DATES. AFTER R.H. DALE (1974).

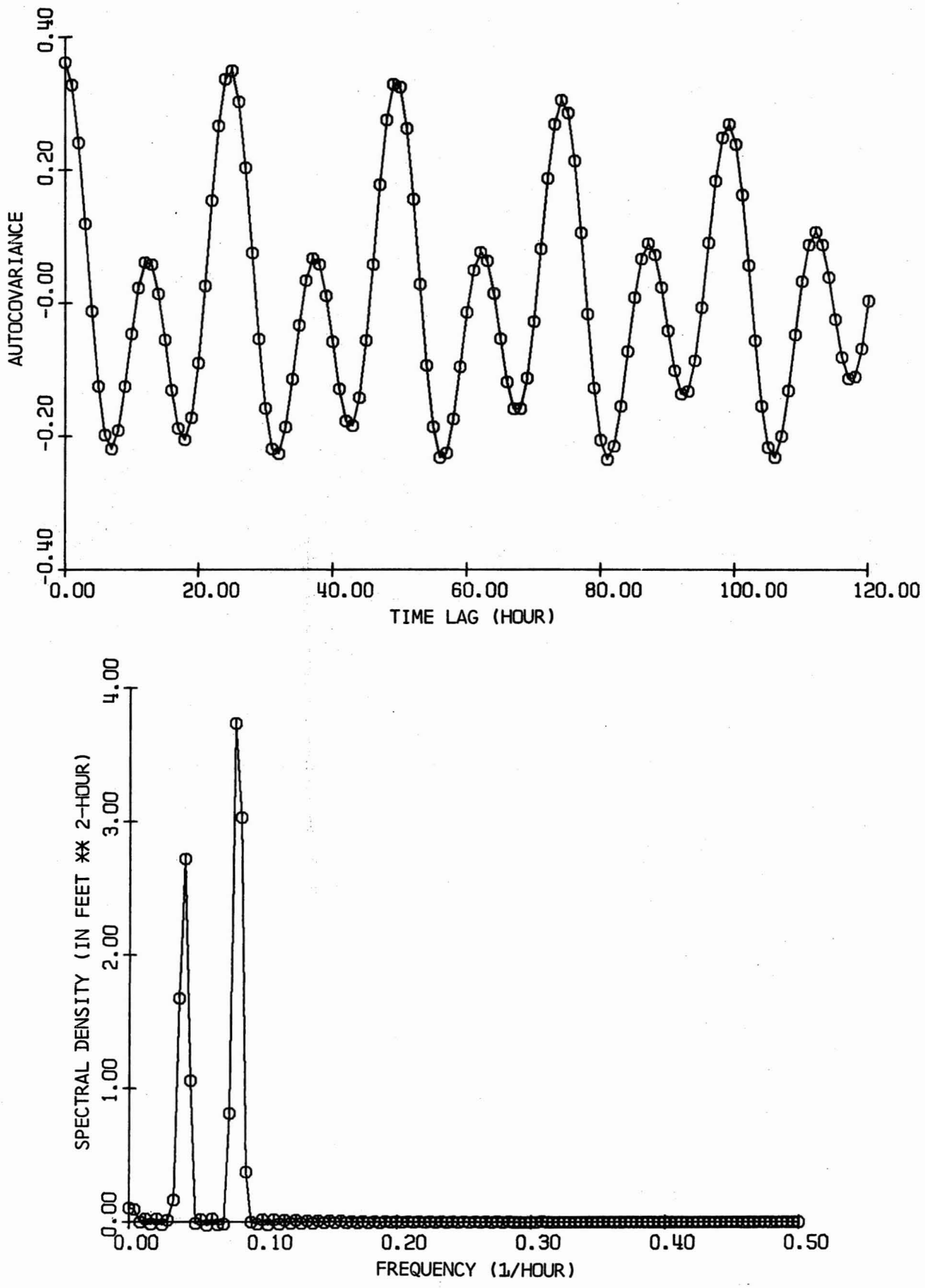

FIGURE 12. AUTOCOVARIANCE vs. TIME LAG AND SPECTRAL DENSITY vs. FREQUENCY FOR THE WATER SURFACE-TIME HISTORY AT HONOLULU HARBOR

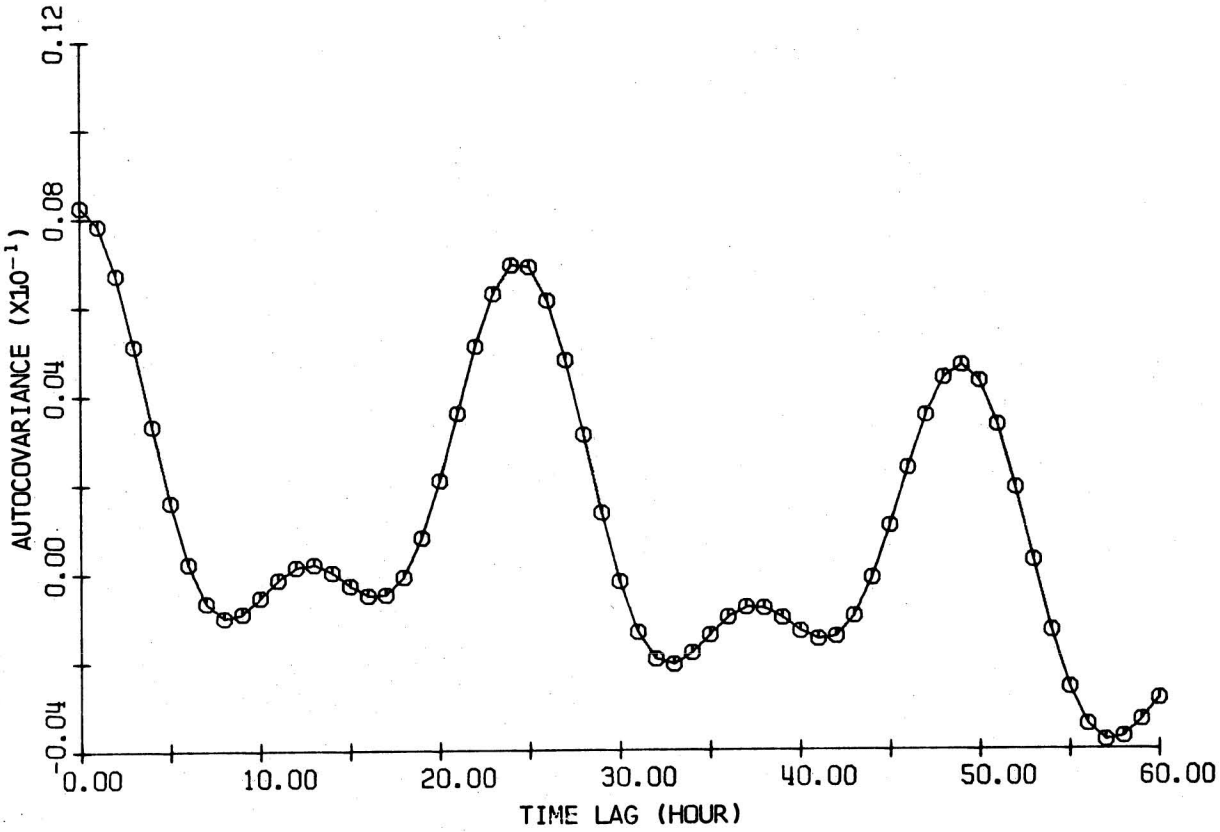

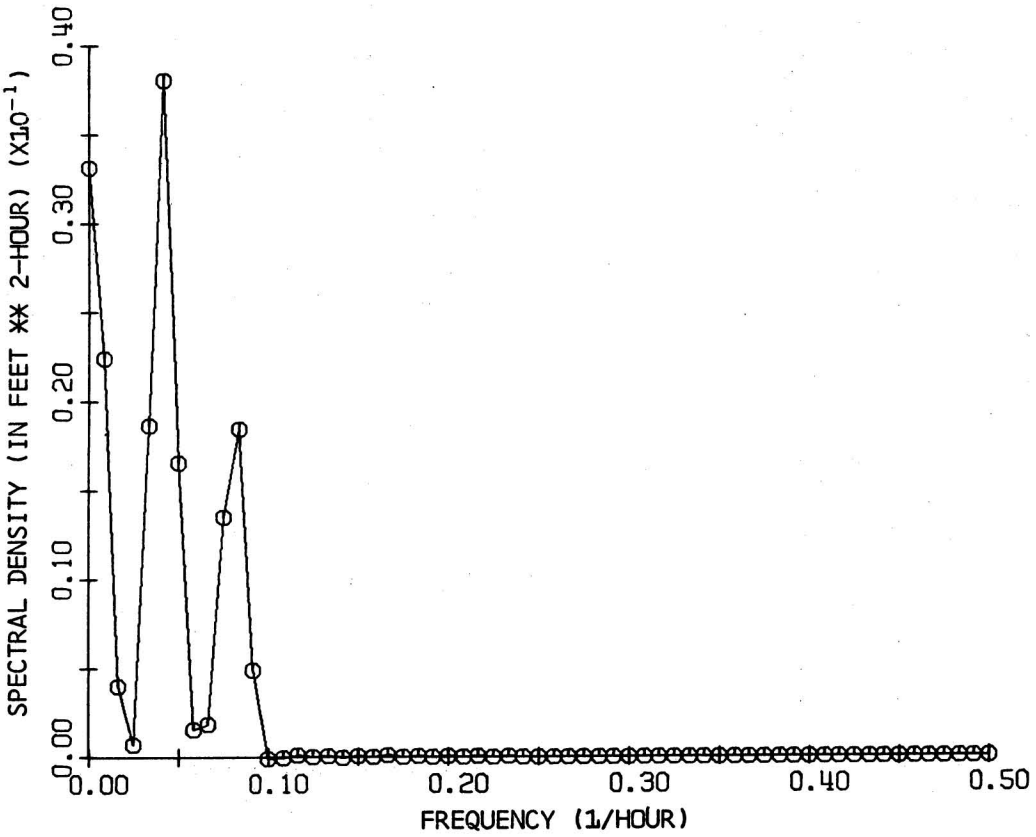

FIGURE 13. AUTOCOVARIANCE vs. TIME LAG AND SPECTRAL DENSITY vs. FREQUENCY FOR THE WATER SURFACE-TIME HISTORY AT DUG WELL NO. 40

TABLE 3. A COMPARISON OF INCIDENT AND TRANSMITTED POWER

SEGMENT OF RECORD	LOCATION	$1/2 \sum_{p=1}^{2} (a_p^2+b_p^2)$, ft^2
PERIODOGRAM ANALYSIS		
5 PM: 27 AUGUST 1965	HONOLULU HARBOR	4039.07×10^{-4}
to	DUG WELL NO. 40	40.00×10^{-4}
5 PM: 28 SEPTEMBER 1965	DUG WELL NO. 41	27.22×10^{-4}
27 AUGUST 1965	HONOLULU HARBOR	4642.24×10^{-4}
	DUG WELL NO. 40	78.22×10^{-4}
	DUG WELL NO. 41	46.12×10^{-4}
28 AUGUST 1965	HONOLULU HARBOR	3484.14×10^{-4}
	DUG WELL NO. 40	40.07×10^{-4}
	DUG WELL NO. 41	34.60×10^{-4}
04 SEPTEMBER 1965	HONOLULU HARBOR	2955.90×10^{-4}
	DUG WELL NO. 40	69.59×10^{-4}
	DUG WELL NO. 41	45.98×10^{-4}
05 SEPTEMBER 1965	HONOLULU HARBOR	2608.38×10^{-4}
	DUG WELL NO. 40	60.72×10^{-4}
	DUG WELL NO. 41	36.58×10^{-4}
06 SEPTEMBER 1965	HONOLULU HARBOR	2935.35×10^{-4}
	DUG WELL NO. 40	67.44×10^{-4}
	DUG WELL NO. 41	34.56×10^{-4}
AVERAGE POWER†	HONOLULU HARBOR	3325.20×10^{-4}
	DUG WELL NO. 40	63.20×10^{-4}
SPECTRAL ANALYSIS		
01 AUGUST 1965 TO 30 SEPTEMBER 1965	HONOLULU HARBOR	3600.00×10^{-4}
26 AUGUST 1965 TO 08 SEPTEMBER 1965*	DUG WELL NO. 40	62.68×10^{-4}

† THE AVERAGE VALUES DO NOT INCLUDE THE "POWER" ESTIMATED FOR 27-28 AUGUST 1965.

* THE POWER ASSOCIATED WITH PERIODS LONGER THAN 24 HOURS (SEE FIGURE 13) IS NOT INCLUDED IN THIS TOTAL.

ing in which to fit the 1/2 watt carbon resistors (± 10% tolerance) and the 50 WVDC ceramic capacitors (± 10% tolerance). Values of 1000 ohms and 0.1 x 10^{-6} farads were selected as the typical electrical sizes for the resistors and capacitors, respectively. These values represent the resistivity, (i.e., the reciprocal of the transmissivity) and storativity, respectively, of one complete grid square. Values of resistance and capacitance for partial grid squares located along the boundaries were determined by the vector area technique (Karplus 1958). The coastline from Brown's Camp to the Salt Evaporators formed the boundary along which the head fluctuated with the tide while at the interior a no-flow boundary was constructed.

The time scale factor (Walton and Prickett 1963), K_4, for the model is

$$K_4 = \frac{a^2(S/T)}{RC} = 4 \cdot 10^{10}(S/T) \text{ days/sec} \qquad (16)$$

where transmissivity, T, is expressed in sq fpd.

At the outset, modeling the wells appeared to pose a problem since the wells possess a characteristic phase lag and amplitude decay factor dependent upon their geometry and independent of the tide.[1] Subsequently, two separate techniques were employed. The first approach was to model the well electrically by constructing a separate electric analog model for the surface layer (approximately 10 ft thick) of that grid square which contained the well. This subsidiary surface model had a refined grid spacing of a = 200 ft, and the well was represented by a single wire shaped to the general geometry of the real well and provided a direct electrical short between those resistors representing the region traversed by the well.

The design of the subsidiary surface model was based on an average aquifer depth of 150 ft and an average well (channel) depth of 10 ft or 6.5% of the average depth. The resistance per square of the surface layer is then $R_2=(h/h_2)R=1000/.065=15{,}500$ ohms and the resistance per square of the base layer is $R_1=(h/h_1)$ 1000=100/.935=1070 ohms. If the typical resistors of R=1000 ohms bounding the grid square containing the well are replaced with resistors of value R_1 ohms, that square and one-half of the square adjacent to each of its sides will represent a section of aquifer thickness, h_1. The numerical value of R_1=1070 ohms is well within the 10% tolerance of resistor, R. Hence, in the basic model, the resistors for the grid square

1. Carr and van der Kamp (1969) used correction factors derived by M.J. Hvorslev (1957).

containing the well were left at R ohms. The subsidiary surface model consisted of 15,500 ohm resistors on the interior and 31,000 ohm resistors along the boundaries of the square. In order to distribute the head around the boundary of the subsidiary surface layer, a second set of 3100-ohm resistors was placed in parallel with each of the boundary resistors of the surface model. This second set of resistors simulates the influence of the surface layer directly adjacent to the grid square which contains the well. To connect the subsidiary surface model, terminals at the corner grid points were connected at the grid points of the square on the basic model which contained the well. The steps outlined above are defined in Figure 14.

The storativity of both the surface and the underlying regions remained concentrated in the capacitors connected at the grid points of the basic model. The storativity of the channel itself was accounted for by a small capacitor whose electrical size was determined from the proportion

$$\frac{C_w}{(\text{surface area})_{well}} = \frac{C}{a^2 S} \tag{17}$$

The surface area of Dug Well No. 40 is estimated at 18,750 sq ft and the storativity at a conservative value of .02, which results in approximately 3 μμf for C_w. (This value is small and had no observable influence on the model output.)

The second technique for estimating the lag time and decay factors for the well channels is based on analytical considerations. Assuming that the changes in elevation of the phreatic surface near the well are approximated by a series of steady state flows leads to the following relations for the amplitude decay and the time lag:[1]

$$\zeta/\zeta_o = 1/[\,1 + (bx_o/(2T)\sigma]^{1/2} \tag{18a}$$

$$\tan \theta_p = -[\,bx_o/(2T)\sigma] \tag{18b}$$

In these equations b is the width of the channel, T the transmissivity, σ the tidal frequency, and x_o the distance from the channel bank beyond which no influence of the channel is observed as the level of the phreatic surface rises or falls. The distance x_o may be estimated from the relation

$$x_o = F\sqrt{thK/\varepsilon'} \tag{19}$$

1. Derivation details of the two factors are given in Appendix A.

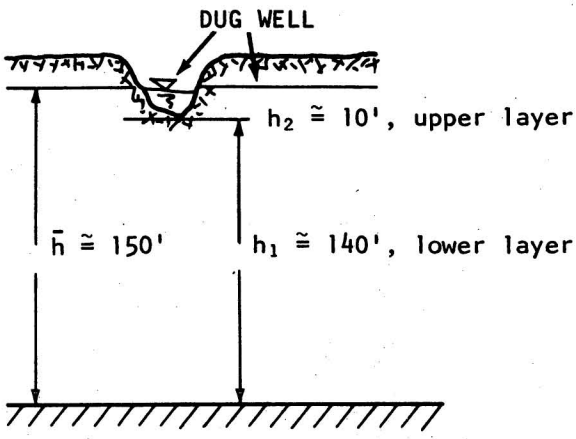

14a. AQUIFER CROSS SECTION

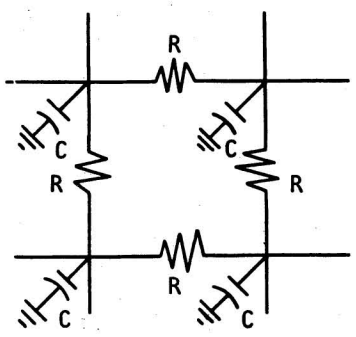

$R = 1000\Omega$, $C = 0.1 \times 10^{-6}$f

14b. TYPICAL GRID SQUARE

$R_1 = \frac{h}{h_1} R = 1070\Omega$

The outlined region represents the lower layer of aquifer, i.e. $h_1 \cong 140'$, modeled by the four resistors, R_1.

Note: $R_1 - R < 0.1R = 100\Omega$

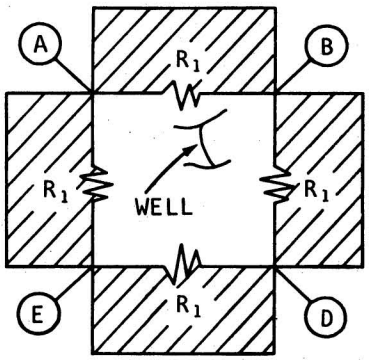

14c. GRID SQUARE CONTAINING WELL

$R_2 = \frac{h}{h_2} R = 15{,}500\Omega$

These resistors, $2R_2/10 = 3100\Omega$, distribute the voltage from the adjacent upper layer, i.e. that portion of the upper layer delineated by crosshatching on 14c.

Subsidiary surface model is connected to basic model by connecting similarly identified pairs of lead wires.

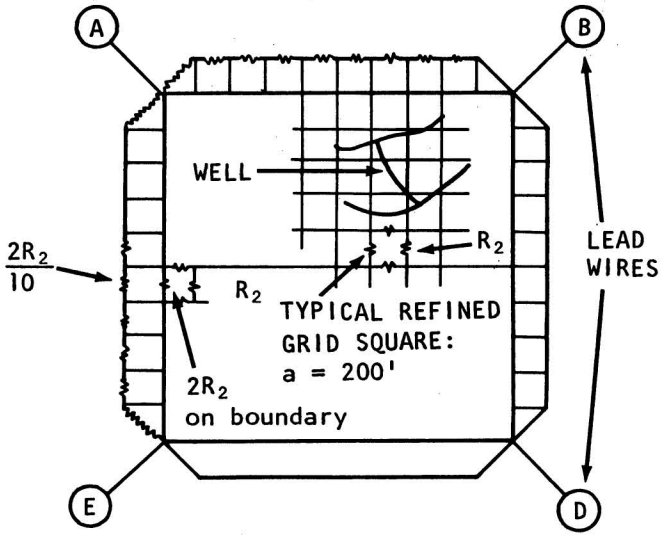

14d. SUBSIDIARY SURFACE MODEL

FIGURE 14. DESIGN OF THE SUBSIDIARY SURFACE MODEL

where t is one-fourth the tidal period, ε' is an effective porosity, and F is a function of time whose value falls in the range $1.23 \leq F \leq 1.73$.[1] The upper and lower bounds of F represent the limiting case where a phreatic aquifer drains into a empty channel and the limiting case where a full channel discharges to an aquifer whose depth is zero at distances $x \geq x_o$ from the channel, respectively. Equation (19) assumes that the bottom of the channel and that of the aquifer coincide. In the case where the aquifer extends below the channel, some flux can be expected to pass through the channel bottom; however, the assumption of no flow through the bottom is entirely consistent with the shallow aquifer theory assumed here. Hence, equation (19) with the depth of the channel $h = h_2$ and $F = 1.73$ should give a reasonable estimate for an upper bound on x_o. Selecting $t = 1/2$ day, $h = 10$ ft, $K = 10^5$ ft/day, $\varepsilon' = 0.1$ results in an $x_o = 340$ ft, and, subsequently, $\theta_p < 1^0$ and $\zeta/\zeta_o << .01$. Thus, from analytic considerations, the presence of the well apparently does not influence significantly the response of the piezometric surface. It is worth noting that x_o may either be doubled or halved and the above inequalities for θ_p and ζ/ζ_o will still be satisfied.

MODEL DATA: ACQUISITION AND ANALYSIS. Data were acquired using the basic model both in conjunction with the subsidiary surface model for Dug Well No. 40 and without it. The electric analog model was driven by a General Radio (No. 1310-A) audio oscillator and the output from the model monitored on a Hewlett-Packard dual trace (No. 122A) oscilloscope: one trace indicating the tidal oscillation at the coastline and the other trace monitoring the response at any selected nodal point. The procedure followed was the same for both model configurations. The time scale factor, K_4, was varied from approximately 600 to 6000 days/sec and the amplitudes and phase angle recorded from the traces on the oscilloscope screen for both the fundamental and second harmonic components (i.e., for the diurnal and semidiurnal components of the tide). The data is recorded in Table 4 where the amplitudes have been normalized with respect to the tidal amplitude at the coast. The dimensionless amplitudes and the phase angles are also plotted as functions of the time scale factor, K_4, and are shown in Figures 15 and 16. It should be noted that when the subsidiary surface model was not used, the

1. Equation (19), derived J. Bear et al. (1968) is based on the assumption that flow can be considered as a series of steady state flows.

TABLE 4. SUMMARY OF DATA FOR ELECTRIC ANALOG MODEL

DUG WELL NO. 40					DUG WELL NO. 41				
SUBSIDIARY SURFACE MODEL DISCONNECTED									
K_4 day/sec	ρ_D	ρ_S	$\theta_{p,D}$ deg	$\theta_{p,S}$ deg	K_4 day/sec	ρ_D	ρ_S	$\theta_{p,D}$ deg	$\theta_{p,S}$ deg
5980	.044	.023	135	210	5980	.013	.017	276	252
598	.392	.266	54	72	598	.366	.183	96	138
2800	.125	.049	101	133	2800	.042	.013	207	265
1780	.200	.096	53	109	1780	.100	.027	107	229
SUBSIDIARY SURFACE MODEL FOR DUG WELL NO. 40 CONNECTED									
5980	.063	.027	102	150	5980	.014	.017	270	246
598	.425	.313	48	60	598	.375	.175	96	135
3500	.125	.050	90	114	3500	.030	.013	220	264
2500	.175	.089	78	90	2500	.048	.017	192	258
5980	.063	.022	99	127	5980	.013	.014	237	246
5980	.044	.018	141	192	5980	.013	.013	264	246
598	.425	.310	44	57	598	.400	.196	86	121
598	.380	.270	52	68	598	.375	.173	96	137
3500	.125	.050	84	104	3500	.029	.013	194	249
3500	.098	.033	112	144	3500	.025	.010	222	273
2500	.178	.083	76	92	2500	.055	.022	167	216
2500	.145	.075	97	124	2500	.049	.014	192	256
1850	.198	.089	83	112	1850	.100	.026	147	199
2750	.135	.050	100	130	2750	.040	.012	210	280

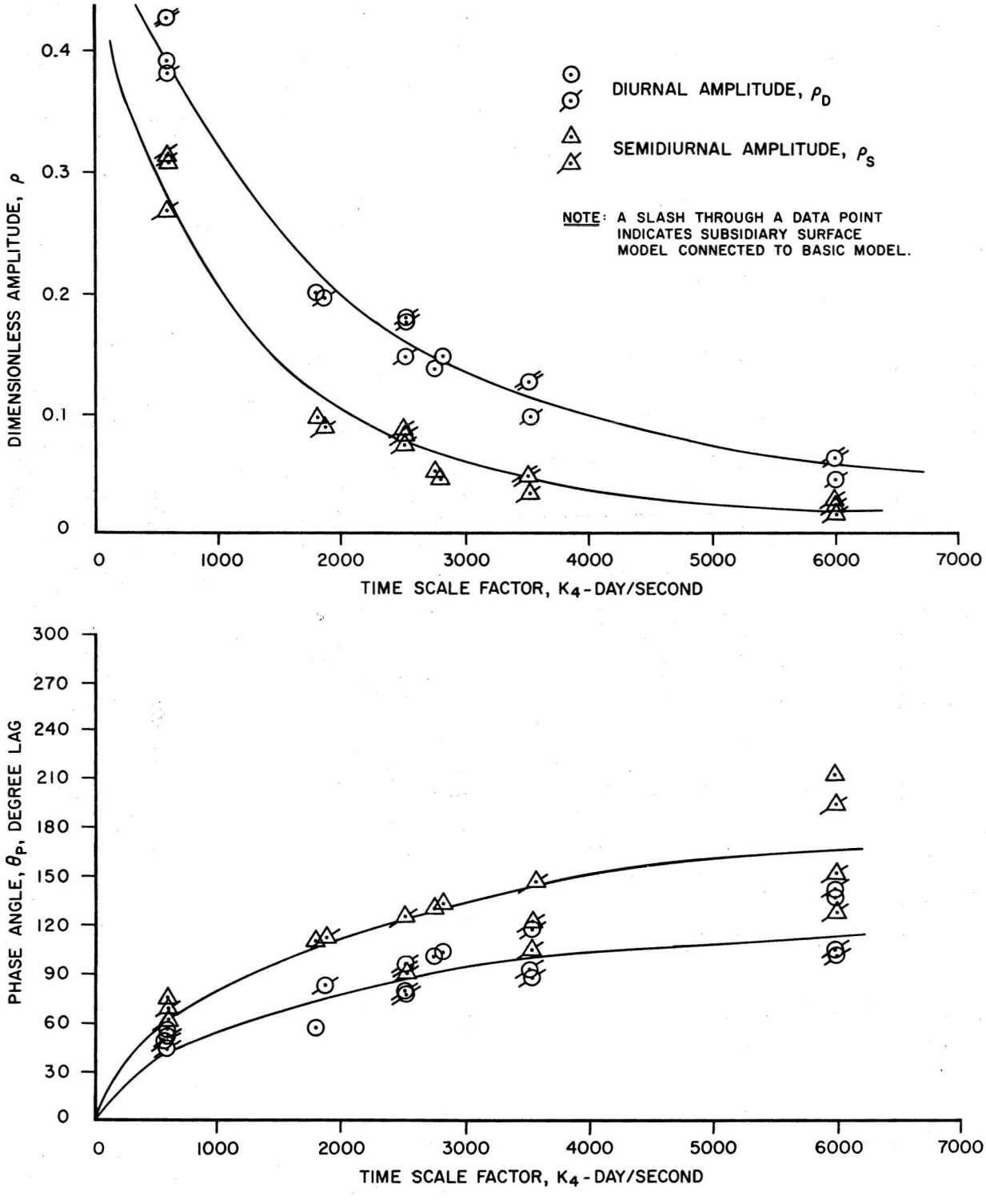

FIGURE 15. DIMENSIONLESS AMPLITUDES, ρ, AND PHASE ANGLES, θ_p, vs. TIME SCALE FACTOR, K_4, FOR THE DIURNAL AND SEMIDIURNAL TIDAL COMPONENTS AT DUG WELL NO. 40

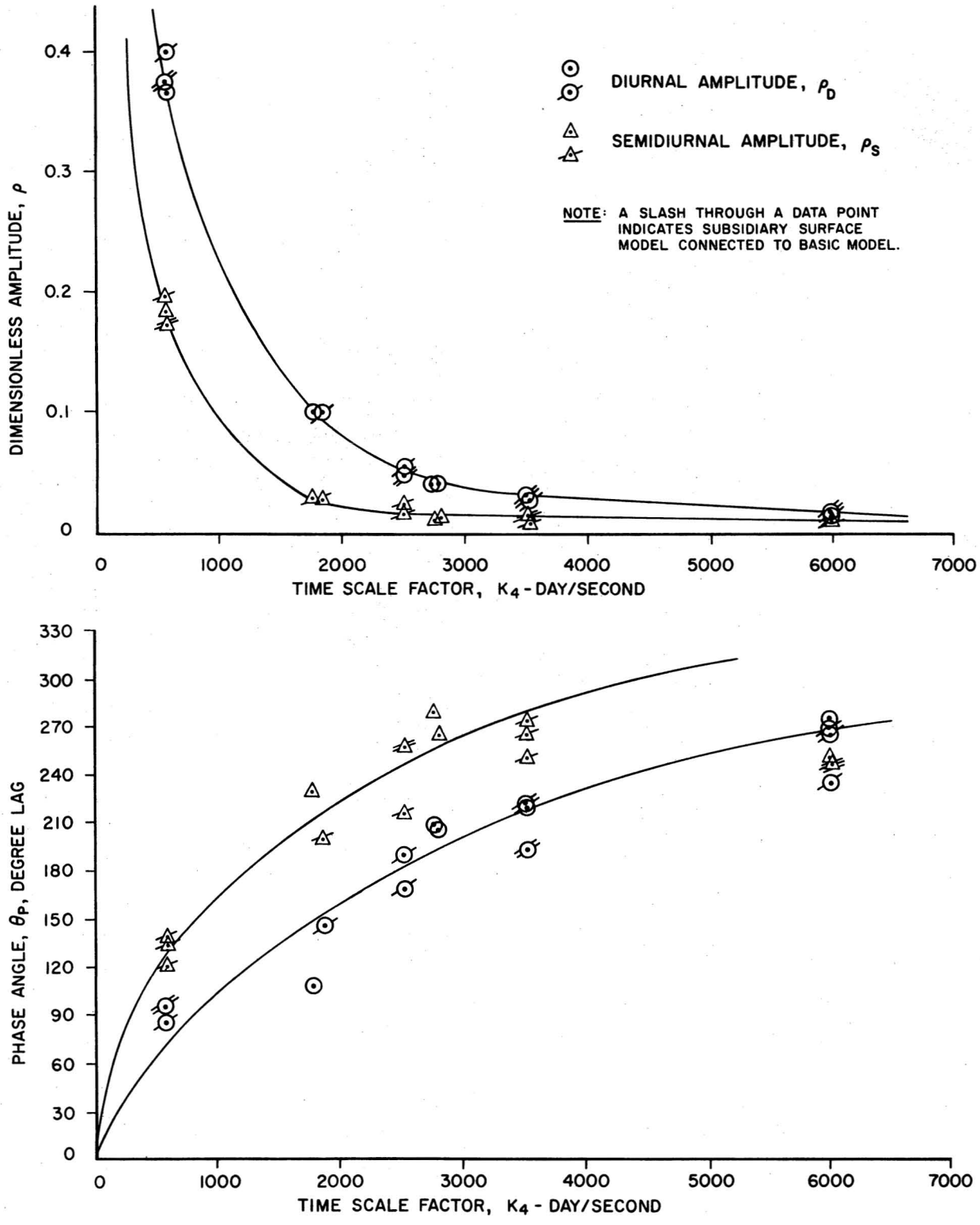

FIGURE 16. DIMENSIONLESS AMPLITUDES, ρ, AND PHASE ANGLES, θ_p, vs. TIME SCALE FACTOR, K_4, FOR THE DIURNAL AND SEMIDIURNAL TIDAL COMPONENTS AT DUG WELL NO. 41

model response was measured at the nodal point nearest the well being monitored.

From the amplitude plots in Figures 15 and 16, it is clear that the subsidiary surface model produces results which are not significantly different from those of the basic model alone, as predicted by the analysis in the previous section. The plots of the phase angles observed on the basic model define relatively good curves, while the phase angles from the combined model show considerable scatter. However, the scatter appears to be more the result of experimental error than a difference in trends between the two sets of data. For the phase angle measurements, the least count on the oscilloscope screen was 12°. Also, the subsidiary model seemed to generate some instability in the basic RC circuit which could easily account for the scatter.[1]

It is also clear from Figures 15 and 16 that different time scale factors are required to produce the observed amount of damping of the two tidal components. This discrepancy raises the question of the influence of the wedging effect caused by the aquifer thickness decreasing by a factor of approximately one-half between the coastline and the interior boundary.

The Influence of Changing Aquifer Thickness

ONE-DIMENSIONAL APPROXIMATION OF THE ELECTRIC ANALOG MODEL. The aquifer region observed in a plan view shows a fair amount of variation in width with Dug Well No. 40 being located at one end of the narrower section approximately halfway between the entrance to Pearl Harbor and Barbers Point. This narrow portion persists for a distance of 4 or 5 miles and suggests that the aquifer model may behave in an essentially one-dimensional manner in this region. To establish this behavior, amplitudes and phase angles were measured at each nodal point along the cross section passing closest to Dug Well No. 40. These data are plotted in Figure 15 together with the one-dimensional solution for an aquifer of constant depth and a no-flow interior boundary. The time scale factor was based on $\varepsilon'/\overline{T}=.87\times10^{-7}$ day/sq ft, which yields $\rho_D=.125$ at Dug Well No. 40. The results show excellent agreement between the predicted and ob-

1. The electric analog model should be operated at frequencies which are considerably different from the natural frequency of the RC network. To ascertain the limits on the frequency, the amplitude at Dug Well No. 40 was observed for a set of values of K_4. The results indicate that error can be expected in the observed amplitude for values of $K_4>6$ or 7×10^3 day/sec. The plot of ρ vs. K_4 for these data is shown in Appendix B.

served amplitude but the observed phase angles are as much as 30% smaller than the predicted values. The observed phase angle data do conform to the general geometry of the theoretical curves, however, and the results are considered to be sufficiently good to justify the use of the one-dimensional flow theory in studying the wedging effect on the aquifer response to tides.

ONE-DIMENSIONAL WEDGING EFFECT. As mentioned previously, Williams and Liu (1971) have derived the relation for both the amplitude and phase angle with the position, x/L, for a one-dimensional flow in an aquifer with linearly changing conductivity. These same relations can be applied to the case of a linearly, but slowly varying thickness, z(x), by utilizing the transmissivity instead of the conductivity to calculate a modified diffusion coefficient, α_1.

The computer program VAMP-NF (Williams and Liu 1971), written specifically to evaluate the output of the mathematical model, would not converge for the relatively large values of α_1, because the terms in the power series representation of the serveral modified Bessel functions became too large. Subsequently, a second computer program was written. This program employed an asymptotic representation of the modified Bessel functions which is valid for arguments greater than or equal to 8 (McLachlan 1934, p. 152). The steps required to calculate the coefficient α_1, together with the new program and a sample output, are included in Appendix C.

To determine what influence the wedging effect had on the aquifer response, the mathematical model was used to evaluate the dimensionless amplitude ρ at x/L=0.6, the relative position of Dug Well No. 40, over the range $0.50 \leq (\varepsilon'/\overline{T}) \times 10^7 \leq 1.25$ for z_L/z_0 equal to 1, 1.2, 1.5, 2, 3, 4, and 5 and for both the diurnal and semidiurnal tides. The results of this evaluation are shown in Figure 18. The mathematical model was also used to compute the amplitudes and phase angles as functions of x/L for $\varepsilon'/\overline{T}=.87\times10^{-7}$ day/sq ft and z_L/z_0=2 and 4. These results have been included in Figure 17 for comparison with those for z_L/z_0=1.

It is seen from Figure 17 that as the ratio of z_L/z_0 increases, the amplitude does not decay as rapidly while the phase angles tend to decrease at a given x/L. This trend holds for both the diurnal and semidiurnal tides. From Figure 18, it is clear that the ratio of the amplitudes at x/L=0.6 for the two tidal components remains essentially constant with respect to variations in z_L/z_0. For example, the ratio is .125/.053 for values of z_L/z_0=1,

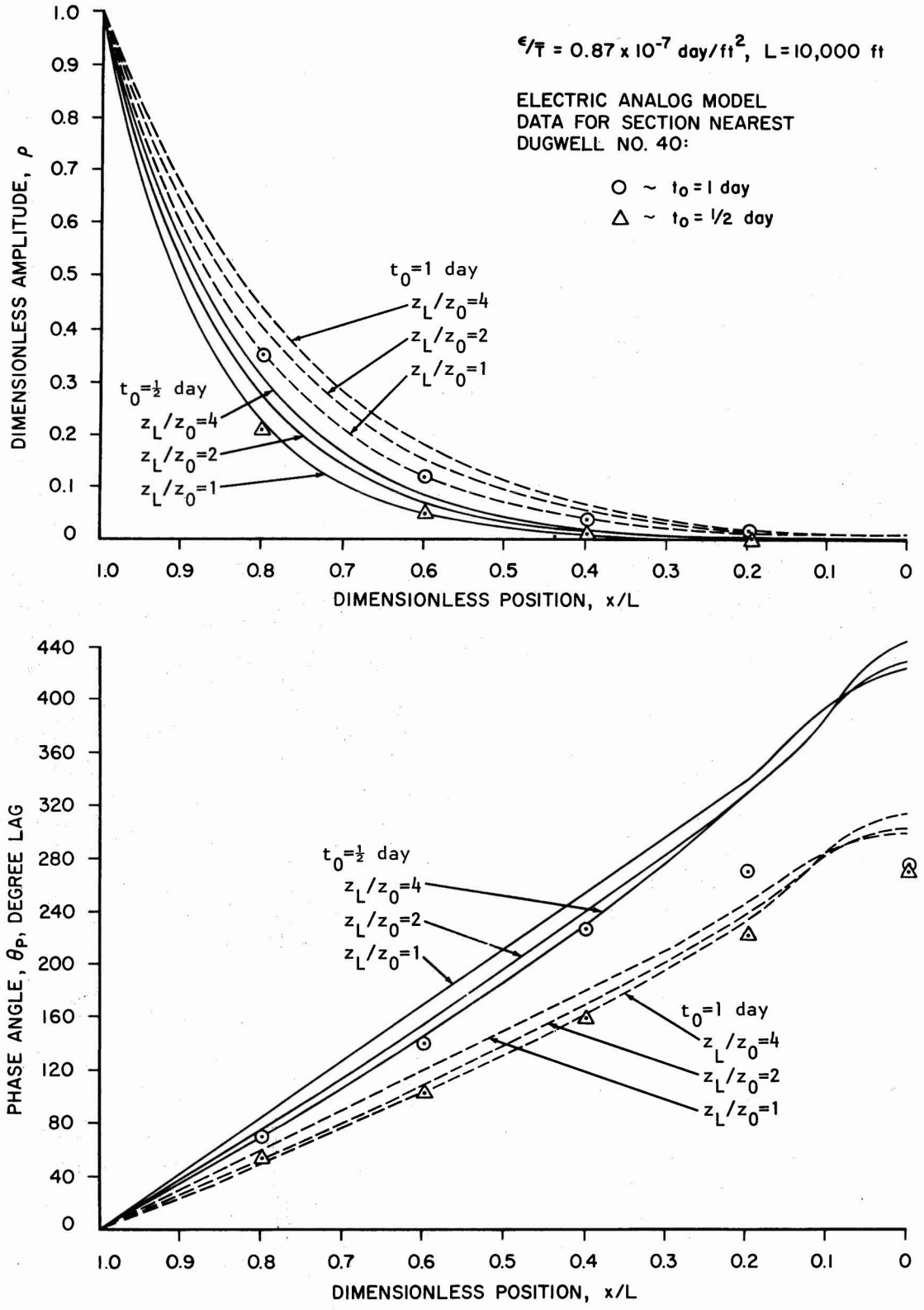

FIGURE 17. DIMENSIONLESS AMPLITUDES, ρ, AND PHASE ANGLES, θ_p, vs. x/L FOR FINITE AQUIFER OF VARIABLE THICKNESS: z_L/z_0 = 1,2,4; $\epsilon'/T = .87 \times 10^{-7}$ day/sq ft AND TIDAL PERIODS OF ONE AND ONE-HALF DAY

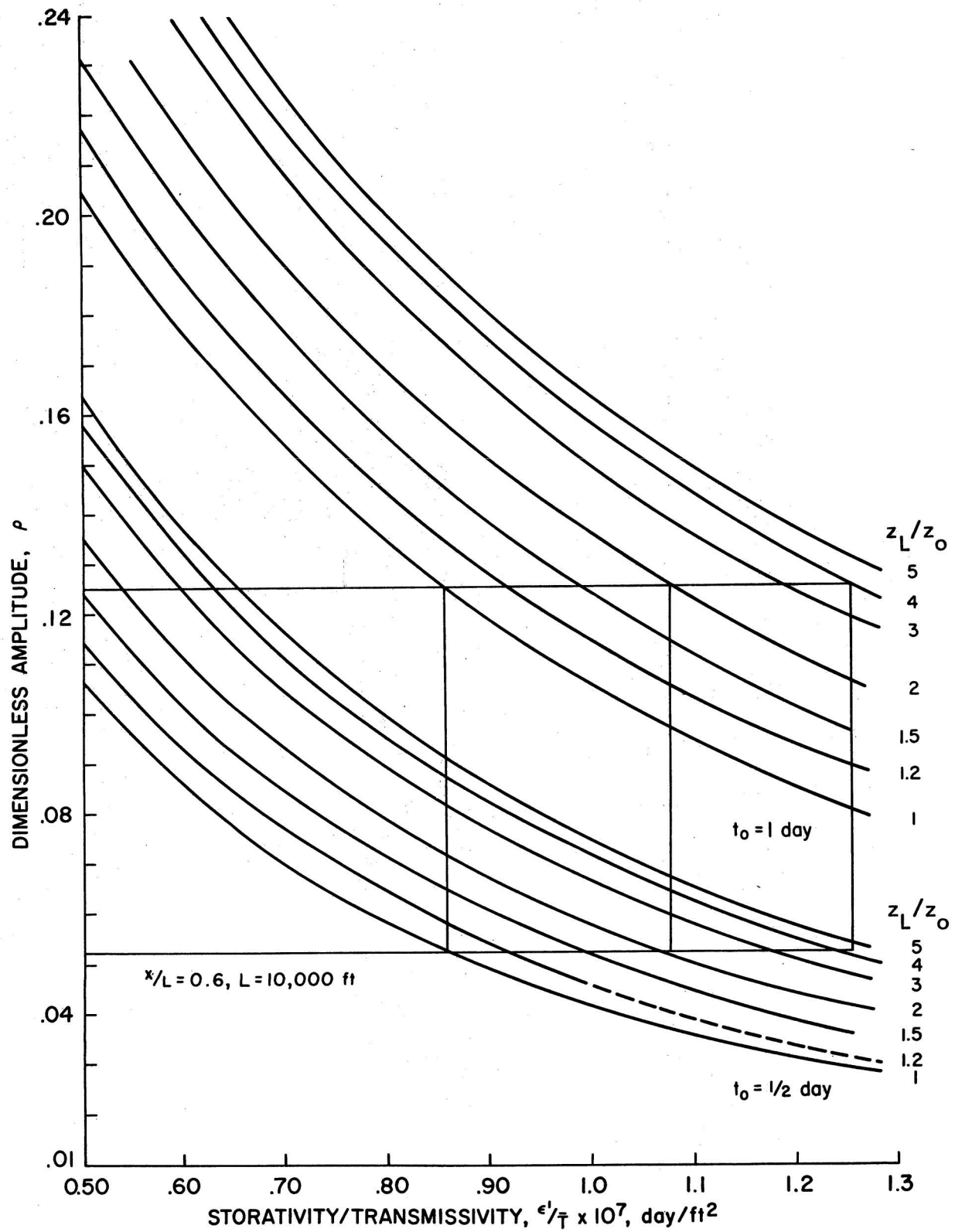

FIGURE 18. DIMENSIONLESS AMPLITUDES, ρ, vs. $\varepsilon'/T \times 10^7$ day/sq ft AT $x/L = 0.6$ FOR $z_L/z_0 = 1, 1.2, 1.5, 2, 3, 4, 5$; AND TIDAL PERIODS OF ONE AND ONE-HALF DAY

2, and 4 while $\varepsilon'/\overline{T}$ takes on the (approximate) values 0.87×10^{-7}, 1.08×10^{-7} and 1.26×10^{-7} day/sq ft, respectively. Thus if it is required that the aquifer exhibit the same ratio of $\varepsilon'/\overline{T}$ for both the diurnal and semidiurnal components, then for a given diurnal tidal efficiency, ρ_D, the semidiurnal tidal efficiency, ρ_S, is fixed. At the same time, these values of ρ_D and ρ_S remain constant with respect to the wedging factor, z_L/z_0. The electric analog model based on a uniform thickness will give an erroneous value of $\varepsilon'/\overline{T}$ for a wedging aquifer. However, Figure 18 may be used to determine the correct value, i.e., in the above example if $z_L/z_0=2$, the corrected value is $\varepsilon'/\overline{T}=1.08\times10^{-7}$ day/sq ft.

DISCUSSION

Results of Field Data Analyses

HARMONIC ANALYSIS. The results of the field data analyses are summarized in Figures 11, 12, and 13 and in Tables 2, 3, and 5. From Table 2, it is seen that the average of the amplitudes a_D and a_S and the relative phase angles θ_D and θ_S are in reasonable agreement with those of Dale (1974)[1] based on a 28-day record. A comparison of the values of the dimensionless amplitudes, ρ_D and ρ_S, and phase angles, $\theta_{p,D}$ and $\theta_{p,S}$, with the averages for those quantities is presented in Table 5. There is a good degree of consistency between the results for each of the five 24-hr segments of the record and again, the average values are in reasonable agreement with those obtained by Dale (1974), particularly for Dug Well No. 41. The standard deviations indicate that two-thirds of the time both ρ_D and ρ_S are within 10% of their average value, while $\theta_{p,D}$ and $\theta_{p,S}$ are within 16% of their average values, except $\theta_{p,S}$ at Dug Well No. 40 where the standard deviation is about 30%. It should be pointed out that the harmonic analysis for the 24-hr period starting from 5:00 P.M. on 27 August 1965, was not included in the average since the trigonometric polynomial for this period produced a poor fit with the given record. This is the result of a poor choice of

1. The daily variations of ρ and θ are the result of both the diurnal and the semidiurnal tidal constituents having slightly different periods and phases which produce the spring and neap tides and cause a beat in the tidal record. For the diurnal constituents, K_1 and D_1, the period of the beat is 13.66 days and for the semidiurnal constituents, M_2 and S_2, the period is 14.785 days.

TABLE 5. COMPARISON OF TIDAL EFFICIENCIES AND PHASE ANGLES

DUG WELL NO.	ρ_D	ρ_S	$\theta_{p,D}$ deg	$\theta_{p,S}$ deg	DATE OF RECORD
FIELD DATA[a]					
40	.085	.104	68.3	66.8	27-28 AUG. 1965
41	.070	.086	88.1	80.5	" " "
40	.217	.089	65.4	68.0	27 AUG. 1965
41	.145	.081	58.7	81.7	" " "
40	.185	.094	59.1	58.3	28 AUG. 1965
41	.168	.088	82.3	80.0	" " "
40	.171	.099	49.0	50.7	04 SEPT. 1965
41	.140	.076	66.7	91.2	" " "
40	.170	.116	46.2	38.8	05 SEPT. 1965
41	.136	.078	74.1	86.5	" " "
40	.178	.114	43.6	24.8	06 SEPT. 1965
41	.131	.075	75.8	89.4	" " "
40	.184	.102	52.7	48.1	AVG. VALUES
41	.144	.080	71.5	85.8	" "
40	.017	.011	8.3	15.1	STD. DEVIATION
41	.013	.005	8.2	4.3	" "
ELECTRIC ANALOG MODEL DATA[b]					
40	.184	.090	70	115	FROM: FIG. 13
41	.144	.045	135	195	" " 14
40	.200	.102	77	110	" " 13
41	.200	.080	110	170	" " 14
FIELD DATA AFTER R.H. DALE[c]					
40	.24	.07	58.4	56.7	25 JUNE to
41	.13	.07	89.3	108.2	22 JULY 1965

[a] ENTRIES ARE CALCULATED FROM DATA PRESENTED IN TABLE 2, e.g., FOR DUG WELL NO. 40, 05 SEPT. 1965, ρ_D=.0978/.5753=.170, and $\theta_{p,D}$= 249.74-203.58=46.16.

[b] ENTRIES ARE BASED ON THE DASHED-LINE CURVES FAIRED THROUGH THE DATA OF FIGURES 13 AND 14. THE AVERAGE VALUES OF ρ_D AND ρ_S ARE BOTH USED AS ENTRY POINTS TO THESE FIGURES.

[c] ENTRIES ARE AFTER R.H. DALE 1974. HERE, ρ_D IS BASED ONLY ON C_{28} OR THE P_1 PLUS THE K_1 TIDAL COMPONENT, WHILE ρ_S IS BASED ONLY ON C_{54} OR THE M_2 TIDAL COMPONENT.

starting points, viz., the peak tide on the 27th as 24 hr later the peak tide is about 15% lower, thus presenting a decidedly nonperiodic fluctuation.

SPECTRAL ANALYSIS. The results of the spectral analysis shown in Figures 12 and 13 confirm the fact that the bulk of the incident "power" as well as that transmitted inland is concentrated at the diurnal and semidiurnal frequencies. It is also clear that more dissipation is experienced by the semidiurnal power than the diurnal, as expected.

In particular, the periods at peak power are 24.00 hr and 12.00 hr, for Dug Well No. 40, and 24.00 hr and 12.63 hr for Honolulu Harbor. It should be pointed out that a spectral analysis of the Honolulu Harbor record, based only on the tidal record for the period of 27 August through 7 September resulted in peak power at 12.00- and 24.00-hr periods.

Table 3 indicates that the power estimated from a 24-hr segment of record varies somewhat from day to day for both Honolulu Harbor and Dug Well No. 40, but the average values of the power for the five 24-hr segments of records agree with the results of the spectral analysis to within 8% or less.

Both spectral density functions show some power at periods greater than 24 hr. For Dug Well No. 40, this amounts to approximately 25% of the total power while at Honolulu Harbor it is only 1 or 2% of the total. This is most likely the result of the longer period tidal constituents. In order to resolve the fortnightly tidal component, 4 to 5 months of records are required for analysis.

Results of Electric Analog Simulation

ELECTRIC ANALOG MODEL RESULTS. The results of the electric analog model tests are summarized in Table 4 and in Figures 15 and 16. The significant result from these tests is that different ratios of storativity to transmissivity are required to produce the observed amount of damping of the diurnal and semidiurnal tidal components. From Figures 15 and 16, the range of variation is $.50\text{x}10^{-7} \leq (\varepsilon'/\overline{T}) \leq .55\text{x}10^{-7}$ day/sq ft at Dug Well No. 40 and $.29\text{x}10^{-7} \leq (\varepsilon'/\overline{T}) \leq .36\text{x}10^{-7}$ day/sq ft at Dug Well No. 41. These differences are small but consistent in that the semidiurnal tide yields the smaller value of $(\varepsilon'/\overline{T})$.

EFFECT OF AQUIFER WEDGING. The electric analog model represents an aquifer of uniform thickness, whereas the observed aquifer is known to de-

crease in thickness as it extends inland from the coastal boundary. The possible influence of this changing thickness on the observed amplitudes and phase angles was considered in terms of a "wedging-factor," (z_L/z_o). However, Figure 18 shows that if the same value of $(\varepsilon'/\overline{T})$ is to describe the aquifer for each tidal frequency, then the ratio of (ρ_D/ρ_S) is independent of aquifer wedging. Consequently, the linear wedging theory offers no explanation to the question of the dependence of $(\varepsilon'/\overline{T})$ on frequency. Figure 18 does, however, provide a means of correcting the results from an electric analog model based upon a uniform aquifer thickness for a linear wedging in the prototype.

Applicability of the Method

THE METHOD. The use of tidal response data to estimate the aquifer properties involves two steps. First, the input and response must be measured in the form of water surface-time histories and the harmonic components of the records resolved. Second, the particular relationship between the input and the response whixh produces the best estimate of the ratio of storativity to transmissivity must be selected. The relationship selected depends upon the nature of the boundaries of the aquifer. If the aquifer is one-dimensional and of infinite extent, it takes the form of equation (5a). For more complicated boundaries, e.g., a finite one-dimensional aquifer with a no-flow boundary condition, a more complicated expression must be used. (See Werner and Noreen 1944; Williams, Wada, and Wang 1970.) For general boundaries no closed-form solution is available, and it is necessary to resort to models such as the electric analog or digital model devised by Dale (1974).

The ratio of storativity to transmissivity for the Ewa Beach aquifer, determined by the electric analog model together with the values found by Dale (1974), are presented in Table 6. There is excellent agreement for the results based upon the diurnal tidal efficiency, ρ_D, while those based upon the semidiurnal tidal efficiency, ρ_S, differ by a factor of three with the electric analog model giving the smaller values. Correcting for aquifer wedging increases $\varepsilon'/\overline{T}$ about 30%. It should be recalled that Dale's (1974) digital model is limited to a one-dimensional aquifer while the electric analog model accounts for horizontal (areal) variations in the aquifer boundaries. This additional capability seems to have little influence on

TABLE 6. COMPARISON OF THE RATIO OF STORATIVITY TO TRANSMISSIVITY.

	DIURNAL COMPONENT				SEMIDIURNAL COMPONENT			
			$\varepsilon'/\overline{T}$, day/ft^2				$\varepsilon'/\overline{T}$, day/ft^2	
	ρ_D	K_4 day/sec	$z_L/z_0=1$	$z_L/z_0=2$[a]	ρ_S	K_4 day/sec	$z_L/z_0=1$	$z_L/z_0=2$
DUG WELL NO. 40	0.184	2200	0.55×10^{-7}	0.72×10^{-7}	0.102	2000	0.50×10^{-7}	0.65×10^{-7}
DUG WELL NO. 41	0.144	1450	0.36×10^{-7}	--	0.080	1150	0.29×10^{-7}	--
	AFTER R.H. DALE[b]							
	ρ_D	K/L^2S $(day)^{-1}$	(S/K) day/ft^2	--	ρ_S	K/L^2S $(day)^{-1}$	(S/K) day/ft^2	--
DUG WELL NO. 40	0.24	0.20	0.50×10^{-7}	--	0.07	0.067	1.50×10^{-7}	--
DUG WELL NO. 41	0.13	0.24	0.40×10^{-7}	--	0.07	0.12	$.80\times10^{-7}$	--

[a] VALUE OF $\varepsilon'/\overline{T}$ CORRECTED FOR WEDGING EFFECT FROM FIGURE 16.

[b] ENTRIES ARE BASED ON ANALYSIS AFTER R.H. DALE 1974. VALUES OF (K/L^2S) HAVE BEEN ESTIMATED FROM TYPE-CURVES OF ρ VS. X/L. L HAS BEEN TAKEN AS 10,000 ft FOR BOTH WELLS.

the model results, however, particularly in the region of Dug Well No. 40, as is evident from Figure 17. Furthermore, the fact that each model yields essentially the same value for the diurnal $(\varepsilon'/\overline{T})$ at Dug Well No. 41 as well as at Dug Well No. 40, indicates that this limitation on the digital model may not be significant for the unconfined Ewa Beach aquifer.[1]

It should be noted, however, that Dale's (1974) results show a considerably greater difference between the diurnal and the semidiurnal storativity-to-transmissivity ratio than does the electric analog model, viz., factors of about 3 and 2 at Dug Wells No. 40 and No. 41, respectively.

VARIABILITY OF THE STORATIVITY-TO-TRANSMISSIVITY RATIO. The experimental results presented in Figures 7 and 8 suggest that the storativity, ε', is weakly dependent or possibly even independent of the period of oscillation for periods greater that a few minutes, say, 15 to 30. The results from the electric analog model show that the diurnal $(\varepsilon'/\overline{T})$ is only 10 to 20% larger than the semidiurnal $(\varepsilon'/\overline{T})$, where the standard deviation on ρ_D and ρ_S is 10%. If Prinz's (1923) observations of tidal fluctuation adjacent to the Elbe River are analyzed on the assumption that equation (5a) is the most appropriate relationship between input and response, the resulting semidiurnal $(\varepsilon'/\overline{T})$ is about 30% greater than the longer period--approximately 9 days--$(\varepsilon'/\overline{T})$.[2] These results suggest that $(\varepsilon'/\overline{T})$ is not basically frequency dependent and that these relatively small differences may be primarily the result of errors in the field measurements or errors in resolving the harmonics present in the time histories of the piezometric surface.

On the other hand, Dale's (1974) results show the semidiurnal $(\varepsilon'/\overline{T})$ to be 100 to 200% greater than the diurnal $(\varepsilon'/\overline{T})$, while van der Kamp (1973) gives the diurnal storativity as 100% greater than the semidiurnal storativity for an unconfined sandstone aquifer at Cap-Pelé, N.B., Canada. van der Kamp (1973) also suggests that the storativity is dependent on frequency with the lower frequencies producing the larger values of storativity.

A comparison of the Ewa Beach and Cap-Pelé aquifer properties with those of the Ottawa sand provides some insight into the dilemma. For the

---

1. Since Dug Well No. 41 is approximately the same distance from the Pearl Harbor Channel as it is from the Ewa Beach coast, a one-dimensional representation of the aquifer in this region should be less reliable than in the vicinity of Dug Well No. 40.
2. The fluctuations at the river bank were excluded from these calculations.

Cap-Pelé aquifer, van der Kamp (1973) reports the specific yield[1] = .015 and the transmissivity = 280 sq m/day. For the Ewa Beach aquifer, the specific yield is estimated to be 0.2 while the conductivity is estimated to be 1.1 $x10^4$ fpd.[2] For the average aquifer thickness of 150 ft, the transmissivity is $1.7x10^6$ sq fpd or $1.5x10^5$ sq m/day. The Ottawa sand used in the experiments described above has a specific yield of .34 and a conductivity of 0.42 cm/sec giving a transmissivity of $0.55x10^5$ sq m/day for a 150-ft thick layer. From a comparison of these properties, it is clear that the Ottawa sand and the Ewa Beach limestone are quite similar with respect to the pore volume available for storativity and the ease with which the water may move through the media. Thus, the response to tides of the Ewa Beach aquifer can be expected to be similar to that of the Ottawa sand, and therefore $(\varepsilon'/\overline{T})$ exhibits relatively little, if any, dependence on the tidal frequency. In this instance, a good share of the 10 to 20% difference between the semidiurnal and diurnal values of $\varepsilon'/\overline{T}$ is attributed to errors in the records and/or errors inherent in the harmonic analysis of the data. On the other hand, the significantly smaller values of specific yield and transmissivity for the Cap-Pelé aquifer apparently result in drainage and imbibition characteristics sufficiently different from the Ottawa sand to cause the storativity to show a decided dependence on time--ε' increasing for the lower tidal frequencies. The fact that Dale's (1974) analysis results in the semidiurnal $(\varepsilon'/\overline{T})$ being substantially larger than the diurnal $(\varepsilon'/\overline{T})$ is contrary to both field and laboratory observation and may well be an error.

It is interesting to note that using the values of $(\varepsilon'/\overline{T})$ corrected for wedging and $\overline{T}=1.7x10^6$ sq fpd gives for the diurnal and semidiurnal storativities, $\varepsilon'_D=0.12$ and $\varepsilon'_S=0.11$. Thus, $\varepsilon'_D/\varepsilon=0.31$ and $\varepsilon'_S/\varepsilon=0.28$, indicating that the storativity is, at the most, only slightly dependent on frequency.

The question of the variation of storativity with both the amplitude and the phase of the tidal components may be raised in view of the hyster-

---

1. The specific yield was ascertained by a pump test of 20-hrs duration and would probably increase somewhat for longer periods of pumping. The porosity of the Cap-Pelé sandstone is given as 22%.
2. This value of the conductivity was determined by Khan (1974) for a coral reef limestone aquifer at Waimanalo, on the island of Oahu, which is considered to be similar to the Ewa Beach aquifer. The porosity of coral reef limestone is 0.30 to 0.35.

etic behavior of the available pore space during dewatering and imbibition. However, such variations do not appear to be significant since the amplitude and phases of the diurnal and semidiurnal components varied considerably for the five segments of record analyzed while the tidal efficiencies remained remarkably consistent (see Tables 2 and 5).

COMPARISON WITH PUMP TEST METHODS. The procedure for the evaluation of aquifer properties by means of pump test data is similar to that using tidal response data: an input (a drawdown applied at the well) and a response (a drawdown at an observation well or wells) must be measured, and the appropriate relationship (pump test formula) between the two selected in order to calculate the aquifer properties.

However, no preliminary analysis of the pump test data similar to the resolution of the harmonic components of the tide records is generally required unless the pumped well itself is used as an observation well. In this case, the well losses must be determined and subtracted from the total drawdown at the pumped well. In both methods, a knowledge of the nature of boundaries is required to select the best relationship between input and response. Finally, both methods give values for aquifer properties which are averaged over the distance separating the points of input and response. In general, the two methods will yield different results (van der Kamp 1973). The pump test method probably produces the more reliable results since the observed data usually requires no preanalysis and, in cases of nonequilibrium data, early time drawdown measurements are relatively uninfluenced by boundaries.

However, the two methods can give results which show a similar statistical distribution of the aquifer properties. For example, a pump test of the step drawdown type described by Williams and Soroos (1973)[1] involves five different discharges and three observation wells. The Theim equation was applied and a transmissivity determined for each discharge from the slope of the drawdown vs. distance-to-the-observation well curve. The transmissivities fell in the range $0.28 \times 10^6 \leq T \leq 0.44 \times 10^6$ sq fpd and $T_{avg} = 0.37 \times 10^6$ sq fpd with a standard deviation of 0.059×10^6 sq fpd. From Table 5 and Figure 15, five values of $(\varepsilon'/\overline{T})$ based on the diurnal tidal efficiency

1. Step drawdown pump test conducted 10 October 1965 at the Wilder Avenue Pumping Station, Honolulu, Hawaii.

at Dug Well No. 40 may be estimated. Using $\varepsilon'=0.1$, five values of $\overline{T}$ result which $1.74\text{x}10^6 \leq \overline{T} \leq 2.21\text{x}10^6$ sq fpd, $(\overline{T})_{ave}=1.89\text{x}10^6$ sq fpd and the standard deviation = $0.18\text{x}10^6$ sq fpd.

CONCLUSIONS

In general, the use of tidal response data is a viable means of estimating aquifer properties in coastal areas or in any region where an aquifer is in communication with a body of water whose free surface is subjected to periodic fluctuations. The technique requires essentially the same amount of field work as a pump test and can be expected to produce results which are generally not as reliable as those from a pump test. A knowledge of the nature of the boundaries, the presence of leakage, etc., is important in interpreting results and, as a rule, it is preferable to work with the amplitudes of the oscillations rather than with the phase angles. The optimum procedure for the evaluation of aquifer properties would include analyses of both tidal response and pump test data since one serves as an independent check on the other.

Specific conclusions drawn from the discussion above are summarized.

1. Tidal efficiencies based on an analysis of a 24-hr water surface-time history which considers only one diurnal and one semidiurnal component are reasonably consistent with those based on a 28-day record and composed of two diurnal and three semidiurnal components. It is recommended, however, that several 24-hr segments be analyzed and that care be taken to select 24-hr segments for which the record is essentially periodic (e.g., see the 24-hr period starting 5:00 P.M., 27 August 1965).

2. In the case of a phreatic aquifer, the storativity appears to have some dependence on frequency. This dependence will be weaker or stronger as the specific yield and/or the transmissivity are larger or smaller, respectively. The storativity (i.e., the effective porosity) will generally be only a fraction of the specific yield (about 30% for the Ewa Beach coral limestone). More research is required in this area.

3. The ratio of the diurnal to the semidiurnal tidal efficiency ρ_D/ρ_S is independent of a linear decrease in aquifer thickness, i.e., of the wedging effect, at least for wedging factors $1 \leq z_L/z_0 \leq 5$.

4. The location and geometry of boundaries, the presence of leakage

and the overall geology of the aquifer region are all important in making the correct interpretation and analysis of tidal response data.

5. The tidal response theory provides a viable method for determining aquifer characteristics. The optimum procedure, however, would include analyses of both tidal response and pump test data.

ACKNOWLEDGMENTS

The authors would like to express their appreciation to Dr. R.H. Dale of the U.S. Geological Survey, Honolulu Office for his assistance in obtaining the field data for Dug Wells Nos. 40 and 41 and for his review of the manuscript. We should also like to thank Dr. R.E. Green of the Department of Soil Science, University of Hawaii for his review of and comments on the section dealing with the effective porosity for an oscillating water table.

REFERENCES

Bear, J. 1972. *Dynamics of fluids in porous media.* New York: Elsevier.

———; Zaslavsky, D.; and Irmay, S. 1968. *Physical principles of water percolation and seepage.* Paris: United Nations Educational, Scientific and Cultural Organization.

Blackman, R.B., and Tukey, J.W. 1954. *The measurement of power spectra.* New York: Dover.

Boussinesq, J. 1904. Recherches théoriques sur l'écoulement des nappes d'eau infiltrees dans le sol et sur le débit des sources. *Journal de mathématiques appliquées*, fasc. 1. Paris: Gauthier-Villars.

Carr, P.A., and van der Kamp, G.S. 1969. Determination of aquifer characteristics by the tidal method. *Water Resources Research* 5(5):1023-31.

Carrier, G.C., and Munk, W. 1952. On the diffusion of tides into permeable rock. *Proceedings*, 5th Symposium on Applied Mathematics, Amer. Math. Soc. 89-96.

Dale, R.H. 1974. "Relationship of groundwater tides to ocean tides: A simulation model." Ph.D. dissertation, University of Hawaii.

De Cazenove, E. 1971. Ondes phreatiques sinusoidales. *La Houille Blanche* 7:601-16.

Defant, A. 1958. *Ebb and flow, the tides of earth, air and water.* Ann Arbor: University of Michigan Press.

Doodson, A.T. 1922. The harmonic development of the tide generating potential. *Proceedings*, Royal Society of London (A 100):305-29.

Hvorslev, M.J. 1957. *Time lag and soil permeability in ground water observations.* Bull. No. 36, U.S. Corps of Engineers.

Jacobs, C.E. 1940. One the flow of water in an elastic artesian aquifer. *Transactions, Amer. Geophysical Union* 21:574-86.

———. 1941. Notes on the elasticity of the Lloyd sand on Long Island, New York. *Transactions, Amer. Geophysical Union* 22:783-87.

Karplus, W.J. 1958. *Analog simulation.* New York: McGraw-Hill.

Khan, I.A. 1974. "An electric analog model study of waste water injection at Waimanalo, Oahu, Hawaiian Islands." Master's thesis, University of Hawaii.

Lam, R.K.W. 1971. "Atoll permeability calculated from ocean and groundwater tides." Ph.D. dissertation, University of California, San Diego.

_____, and Liu, T.-C. 1971. *The response to tidal fluctuations of two nonhomogeneous coastal aquifer models.* Tech. Rep. No. 51, Water Resources Research Center, University of Hawaii.

_____, and Liu, T.-C. 1973. *The response to tidal fluctuations of a leaky aquifer system.* Tech. Rep. No. 66, Water Resources Research Center, University of Hawaii.

_____, and Soroos, R.L. 1973. *Evaluation of methods of pumping test analyses for application to Hawaiian aquifers.* Tech. Rep. No. 70, Water Resources Research Center, University of Hawaii.

APPENDICES

Appendix A. Estimate of Response Factors for Dug Wells No. 40 and No. 41

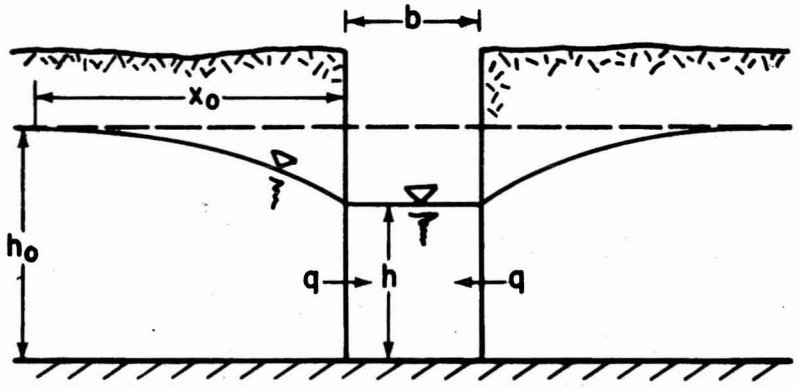

A long, two-dimensional ditch intersects an aquifer in which the elevation of the phreatic surface is subjected to periodic fluctuations. The water surface in the ditch will also fluctuate, but will lag behind the phreatic surface of the aquifer and have a smaller amplitude. This phase lag and amplitude decay are characteristic of the ditch geometry and the media and may be estimated in the following way.

If it is assumed that the oscillations are of sufficiently small amplitude to justify the use of the Dupuit assumptions and the shallow aquifer theory, then $q = -Kh\partial h/\partial x = -K\bar{h}\partial h/\partial x$. This last expression may be integrated and solved for q to give

$$q = K\bar{h}/x_o(h_o-h)$$

The conservation of mass principle applied to the boundaries of the ditch requires that

$$q = b/2\ (dh/dt) \quad .$$

If it is assumed that the rise or fall of the phreatic surface produces a series of steady state flows in to or from the ditch, then q may be eliminated between these last two equations to give

$$bx_o/2K\bar{h}\ (dh/dt) = \alpha\ (dh/dt) = h_o-h;\ \alpha = bx_o/2K\bar{h} \quad .$$

The particular integral for this equation represents the steady state solution. If $h = \bar{h} + \zeta \sin(\sigma t + \theta p)$, then at $x = x_o$, $h_o = \bar{h} + \zeta_o \sin\sigma t$, where x_o is the distance beyond which no influence of the ditch is observed in the

deflection of the phreatic surface. Substituting this solution into the differentiatial equation gives

$$\alpha\zeta\sigma\cos(\sigma t+\theta_p) = \zeta_o \sin\sigma t-\zeta\sin(\sigma t+\theta_p)$$
$$= (\zeta_o-\zeta\cos\theta_p)\sin\sigma t-\zeta\sin\theta_p\cos\sigma t\ .$$

or

$$\cos\theta_p-\alpha\sigma\sin\theta_p = \zeta_o/\zeta$$
$$\alpha\sigma\cos\theta_p + \sin\theta_p = 0$$

This last pair of equations may be solved for θ_p and ζ/ζ_o, i.e.,

$$\tan\theta_p = -\alpha\sigma$$
$$\zeta/\zeta_o = 1/[1/\sqrt{1+(\alpha\sigma)^2}+(\alpha\sigma)^2/\sqrt{1+(\alpha\sigma)^2}]$$
$$= 1/\sqrt{1+(\alpha\sigma)^2}\ .$$

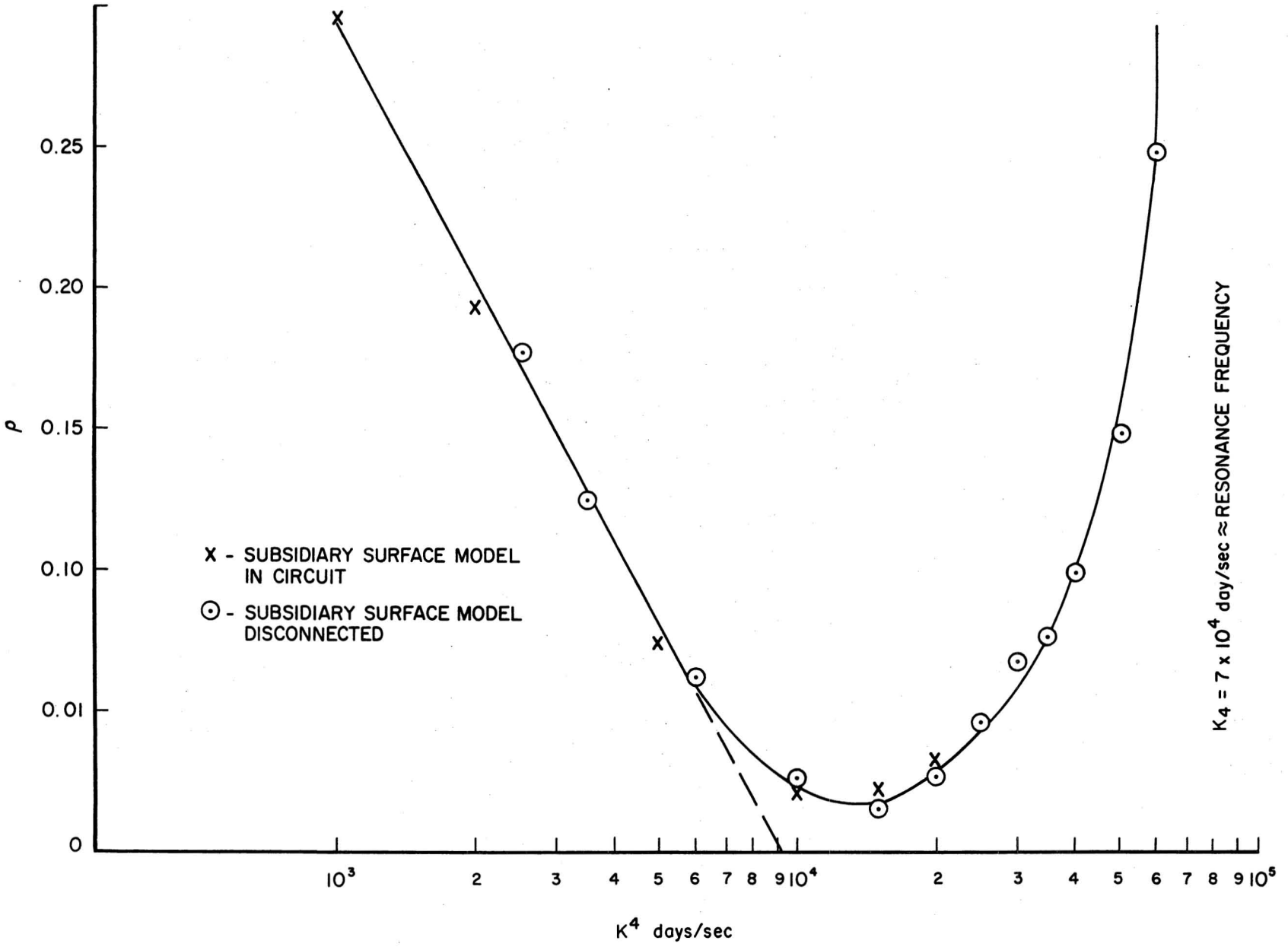

APPENDIX B. RESONANCE FREQUENCY FOR ELECTRIC ANALOG MODEL

Appendix C. Fortran Program for the Evaluation of Variable Permeability Aquifer Model for $\alpha_1 \geq 8$

The mathematical model, VAMP-NF, may be applied to the case of a variable thickness z(x) by making a modification of the coefficient $\alpha = \varepsilon'\sigma/m^2\bar{z}K_0$. Here ε' is the effective porosity, $\bar{z}$ is the uniform thickness of the aquifer, K_0 is the conductivity at the interior boundary, and m is determined from the relation $K(x) = K_0(1 + mx)$ evaluated at $x = L$, the interior boundary. In terms of the transmissivity, this latter expression is $T(x) = T_0(1 + mx)$; $T = \bar{z}K$, and $m = (T_L/T_0 - 1)/L$. If it is the thickness which changes rather than the conductivity, then $m = (z_L/z_0 - 1)/L$. Also, $\overline{T} = (T_0 + T_L)/2 = T_0(1 + z_L/z_0)/2$. Substitution of these last expressions into that for α gives

$$\alpha_1 = \varepsilon'\sigma L^2/2\overline{T} \cdot (1 + z_L/z_0)/(z_L/z_0 - 1)^2$$

$$= \alpha\left[(1 + z_L/z_0)/2\right] \; ; \quad \bar{z}K_0 = \overline{T}$$

The coefficient, α_1, may be substituted into the mathematical model, VAMP-NF, for the determination of ρ and θ as functions of position, x/L. Note that $\overline{T} = \bar{z}K_0$ is now the product of the average thickness and the constant conductivity.

In Figure 18 the smallest value of α_1 occurs for $z_L/z_0 = 5$ and $\varepsilon'/\overline{T} = .50\text{x}10^{-7}$ day/sq ft and is approximately 6. Hence, the curve for $z_L/z_0 = 5$ in Figure 18 may be slightly in error. For the remaining curves, α_1 exceeds 8. In fact, for $z_L/z_0 < 1.2$, the resulting α_1 generates numbers in the asymptotic expansions which cause an "overflow" in the IBM 360.

```
FORTRAN IV G LEVEL  21                MAIN              DATE = 75142        23/00/50

            C     ******************************************************************
            C     VAMP - NF
            C     THIS PROGRAM IS USED TO CALCULATE THE AMPLITUDE AND THE PHASE
            C     ANGLE FOR COASTAL AQUIFER WITH LINEAR INCREASE OR DECREASE IN
            C     HYDRAULIC CONDUCTIVITY, NO FLOW AT INTERNAL BOUNDARY.
            C     ******************************************************************
0001                  DOUBLE PRECISION AL, CL, CKL, CKO, M, CD, PERIOD, SIGMA, ALPHA,
                     1       TENX, X, XI, P, PB, P1, BEROP, BEIOP, A12, A1, A2, CKROP,
                     2       CKIOP, A32, A3, A4, BER1PB, BEI1PB, B12, B1, B2, CKR1PB,
                     3       CKI1PB, B32, B3, B4, BEROP1, BEIOP1, C12, C1, C2, CKROP1,
                     4       CKIOP1, C32, C3, C4, A, B, C, D, RI, RXI, RL, RCL, R, RHO,
                     5       SCA, SINA, AS, SCB, SINB, BS, SCC, SINC, CS, SCD, SIND, DS,
                     6       TS, COSA, AC, COSB, BC, COSC, CC, COSD, DC, TC, TAM, THETAP
                     7       , DEGREE, SQ2, PI
0002        10        READ(5,20)PERIOD,CD
0003        20        FORMAT(F15.0,D15.7)
0004                  IF(PERIOD .EQ. 0.0) STOP
0005                  AL=10000.0
0006                  PI=3.1415927
0007                  CL=2.0
0008                  M=(CL-1.0)/AL
0009        1         SIGMA=2.0*PI/PERIOD
0010                  ALPHA=(3.0*SIGMA*CD)/(2.0*M*M)
0011                  WRITE(6,30)PERIOD,CD,CL,ALPHA
0012        30        FORMAT (1H1,9HPERIOD = ,F6.3,5H DAYS/1H0,5HCD = ,D9.3,9HDAY/FT**2/
                     1      1H0,8HZL/ZO = ,F4.2/1H0,8HALPHA = ,D10.4/1H0,8HLOCATION,
                     2      4X,9HAMPLITUDE,7X,11HPHASE ANGLE)
0013                  TENX=20.0
0014        2         X=TENX/20.0
0015                  XI=1.0+(M*AL*X)
0016                  P=DSQRT(4.0*ALPHA*XI)
0017                  PB=DSQRT(4.0*ALPHA)
0018                  P1=DSQRT(4.0*ALPHA*CL)
0019                  SQ2=2.0
0020                  SQ2=DSQRT(SQ2)
0021                  A1=(DEXP(P/SQ2)/DSQRT(2.0*PI*P))*(1.0+1.0/(8.0*SQ2*P)
                     1       +1.0/(256.0*P*P)-133.0/(2048.0*SQ2*(P**3.0)))
0022                  A12=A1*A1
0023                  A2=P/SQ2-PI/8.0-1.0/(8.0*SQ2*P)-1.0/(16.0*P*P)
                     1       -25.0/(384.0*SQ2*(P**3.0))
0024                  A3=DSQRT(PI/(2.0*P))*DEXP(-1.0*P/SQ2)*(1.0-1.0/(8.0*SQ2*P)
                     1       +1.0/(256.0*P*P)+133.0/(2048.0*SQ2*(P**3.0)))
0025                  A32=A3*A3
0026                  A4=-1.0*P/SQ2-PI/8.0+1.0/(8.0*SQ2*P)-1.0/(16.0*P*P)
                     1       +25.0/(384.0*SQ2*(P**3.0))
0027                  B1=(DEXP(PB/SQ2)/DSQRT(2.0*PI*PB))*(1.0-3.0/(8.0*SQ2*PB)
                     1       +9.0/(256.0*PB*PB)+327.0/(2048.0*SQ2*(PB**3.0)))
0028                  B12=B1*B1
0029                  B2=PB/SQ2+3.0*PI/8.0+3.0/(8.0*SQ2*PB)+3.0/(16.0*PB*PB)
                     1       +21.0/(128.0*SQ2*(PB**3.0))
0030                  B3=DSQRT(PI/(2.0*PB))*DEXP(-1.0*PB/SQ2)*(1.0+3.0/(8.0*SQ2*PB)
                     1       +9.0/(256.0*PB*PB)-327.0/(2048.0*SQ2*(PB**3.0)))
0031                  B32=B3*B3
0032                  B4=-1.0*PB/SQ2-5.0*PI/8.0-3.0/(8.0*SQ2*PB)+3.0/(16.0*PB*PB)
                     1       -21.0/(128.0*SQ2*(PB**3.0))
0033                  C1=(DEXP(P1/SQ2)/DSQRT(2.0*PI*P1))*(1.0+1.0/(8.0*SQ2*P1)
                     1       +1.0/(256.0*P1*P1)-133.0/(2048.0*SQ2*(P1**3.0)))
0034                  C12=C1*C1
0035                  C2=P1/SQ2-PI/8.0-1.0/(8.0*SQ2*P1)-1.0/(16.0*P1*P1)
                     1       -25.0/(384.0*SQ2*(P1**3.0))
0036                  C3=DSQRT(PI/(2.0*P1))*DEXP(-1.0*P1/SQ2)*(1.0-1.0/(8.0*SQ2*P1)
                     1       +1.0/(256.0*P1*P1)+133.0/(2048.0*SQ2*(P1**3.0)))
0037                  C32=C3*C3
0038                  C4=-1.0*P1/SQ2-PI/8.0+1.0/(8.0*SQ2*P1)-1.0/(16.0*P1*P1)
                     1       +25.0/(384.0*SQ2*(P1**3.0))
0039                  A=A1*C3*B1*B3
0040                  B=B12*C3*A3
0041                  C=C1*A1*B32
0042                  D=C1*B1*A3*B3
0043                  RI=((A2-B2)-(A4-B4))
0044                  RXI=(B32*A12)+(B12*A32)-(2.0*B1*B3*A1*A3*DCOS(RI))
0045                  RL=((C2-B2)-(C4-B4))
0046                  RCL=(B32*C12)+(B12*C32)-(2.0*B1*B3*C1*C3*DCOS(RL))
0047                  R=RXI/RCL
0048                  RHO=DSQRT(DABS(R))
0049                  SCA=((A2-B2)-(C4-B4))
0050                  SINA=DSIN(SCA)
0051                  AS=A*SINA
0052                  SCB=A4-C4
0053                  SINB=DSIN(SCB)
```

```
0054                BS=B*SINB
0055                SCC=A2-C2
0056                SINC=DSIN(SCC)
0057                CS=C*SINC
0058                SCD=((A4-B4)-(C2-B2))
0059                SIND=DSIN(SCD)
0060                DS=D*SIND
0061                TS=-AS+BS+CS-DS
0062                COSA=DCOS(SCA)
0063                AC=A*COSA
0064                COSB=DCOS(SCB)
0065                BC=B*COSB
0066                COSC=DCOS(SCC)
0067                CC=C*COSC
0068                COSD=DCOS(SCD)
0069                DC=D*COSD
0070                TC=-AC+BC+CC-DC
0071                TAM=TS/TC
0072                THETAP=DATAN(TAM)
0073                IF(TS.GT.0.0.AND.TC.GT.0.0) THETAP=THETAP-2.0*PI
0074                IF(TS.GT.0.0.AND.TC.LT.0.0) THETAP=THETAP-PI
0075                IF(TS.LT.0.0.AND.TC.LT.0.0) THETAP=THETAP-PI
0076                DEGREE=THETAP*(360.0/(2.0*PI))
0077                WRITE(6,40)X,RHO,DEGREE
0078          40    FORMAT(1H0,D9.3,D15.6,D16.6)
0079                IF(TENX.EQ.0.00) GO TO 10
0080                TENX=TENX-1.0
0081                GO TO 2
0082                END

    *OPTIONS IN EFFECT*   ID,EBCDIC,SOURCE,NOLIST,NODECK,LOAD,NOMAP
    *OPTIONS IN EFFECT*   NAME = MAIN     , LINECNT =      58
    *STATISTICS*     SOURCE STATEMENTS =       82,PROGRAM SIZE =     4520
    *STATISTICS*   NO DIAGNOSTICS GENERATED



 F88-LEVEL LINKAGE EDITOR OPTIONS SPECIFIED   NONE
         DEFAULT OPTION(S) USED -  SIZE=(96256,43008)
****USERPROG  DOES NOT EXIST BUT HAS BEEN ADDED TO DATA SET
```

PERIOD = 1.000 DAYS

CD = 0.870D-07DAY/FT**2

ZL/Z0 = 2.00

ALPHA = 0.8200D 02

LOCATION	AMPLITUDE	PHASE ANGLE
0.100D 01	0.100000D 01	-0.203551D-12
0.950D 00	0.801350D 00	-0.130552D 02
0.900D 00	0.640377D 00	-0.262796D 02
0.850D 00	0.510265D 00	-0.396808D 02
0.800D 00	0.405376D 00	-0.532667D 02
0.750D 00	0.321061D 00	-0.670457D 02
0.700D 00	0.253485D 00	-0.810253D 02
0.650D 00	0.199493D 00	-0.952104D 02
0.600D 00	0.156488D 00	-0.109601D 03
0.550D 00	0.122328D 00	-0.124188D 03
0.500D 00	0.952470D-01	-0.138958D 03
0.450D 00	0.737895D-01	-0.153898D 03
0.400D 00	0.567698D-01	-0.169026D 03
0.350D 00	0.432501D-01	-0.184454D 03
0.300D 00	0.325370D-01	-0.200497D 03
0.250D 00	0.241912D-01	-0.217810D 03
0.200D 00	0.180328D-01	-0.237369D 03
0.150D 00	0.140685D-01	-0.259512D 03
0.100D 00	0.121647D-01	-0.281419D 03
0.500D-01	0.116465D-01	-0.297235D 03
0.0	0.116086D-01	-0.302909D 03

PERIOD = 0.500 DAYS

CD = 0.870D-07DAY/FT**2

ZL/Z0 = 2.00

ALPHA = 0.1640D 03

LOCATION	AMPLITUDE	PHASE ANGLE
0.100D 01	0.100000D 01	0.0
0.950D 00	0.729196D 00	-0.184611D 02
0.900D 00	0.529608D 00	-0.371604D 02
0.850D 00	0.383057D 00	-0.561076D 02
0.800D 00	0.275867D 00	-0.753124D 02
0.750D 00	0.197780D 00	-0.947858D 02
0.700D 00	0.141133D 00	-0.114539D 03
0.650D 00	0.100218D 00	-0.134585D 03
0.600D 00	0.707996D-01	-0.154939D 03
0.550D 00	0.497499D-01	-0.175618D 03
0.500D 00	0.347663D-01	-0.196639D 03
0.450D 00	0.241605D-01	-0.218017D 03
0.400D 00	0.166962D-01	-0.239745D 03
0.350D 00	0.114671D-01	-0.261780D 03
0.300D 00	0.780807D-02	-0.284061D 03
0.250D 00	0.523833D-02	-0.306669D 03
0.200D 00	0.343278D-02	-0.330295D 03
0.150D 00	0.221364D-02	-0.356990D 03
0.100D 00	0.153113D-02	-0.287717D 02
0.500D-01	0.131363D-02	-0.577961D 02
0.0	0.129677D-02	-0.690858D 02